

# Initiation of Clockwise Rotation and Eastward Transport of Southeastern Tibet Inferred from Deflected Fault Traces and GPS Observations

Weijun Gan<sup>1,†</sup>, Peter Molnar<sup>2,§</sup>, Peizhen Zhang<sup>1,3,§</sup>, Genru Xiao<sup>4,§</sup>, Shiming Liang<sup>1,§</sup>, Keliang Zhang<sup>1,§</sup>,  
Zhangjun Li<sup>1,§</sup>, Keke Xu<sup>1,§</sup>, and Ling Zhang<sup>1,§</sup>

<sup>1</sup>State Key Laboratory of Earthquake Dynamics, Institute of Geology, China Earthquake Administration, Beijing 100029, China

<sup>2</sup>Department of Geological Sciences and Cooperative Institute for Research in Environmental Sciences, University of Colorado, Boulder, Colorado 80309, USA

<sup>3</sup>Guangdong Provincial Key Laboratory of Geodynamics and Geohazards, Guangzhou, Guangdong 510275, China

<sup>4</sup>Department of Geodesy, East China University of Technology, Nanchang, Jiangxi 330013, China

## ABSTRACT

Eastward transport and clockwise rotation of crust around the southeastern margin of the Tibetan Plateau dominates active deformation east of the Eastern Himalayan Syntaxis. Current crustal movement inferred from GPS measurements indicates ongoing distortion of the traces of the active Red River fault and the Mesozoic Yalong-Yulong-Longmen Shan thrust belt. By extrapolating current rates back in time, we infer that this pattern of deformation developed since  $10.1 \pm 1.5$  Ma. This date of initiation is approximately synchronous with a suite of tectonic phenomena, both near and far, within the wide Eurasia/Indian collision zone, including the initiation of slip on the Ganzi-Yushu-Xianshuuhe fault and crustal thinning and E-W extension by normal faulting on N-S-trending rifts in the plateau interior. Accordingly, the eastward movement of eastern Tibet and the clockwise rotation of that material seem to be local manifestations of a larger geodynamic event at ca. 10–15 Ma that changed the kinematic style and reorganized deformation not only on the plateau-wide scale, but across the entire region affected by the India/Eurasia collision. Convective removal of some or all of Tibet's mantle lithosphere seems to offer the

simplest mechanism for these approximately simultaneous changes.

## INTRODUCTION

Evidence from much of eastern Asia suggests that long after India's collision with Eurasia at ca. 50 Ma, the style of deformation changed since 10–15 Ma. Although the thick crust beneath the Tibetan Plateau resulted from Late Cretaceous and Cenozoic horizontal shortening both before and since India collided with Eurasia (e.g., Kapp and DeCelles, 2019), both fault plane solutions of earthquakes and GPS measurements show that normal faulting, E-W extension, and crustal thinning characterize the latest active deformation within the plateau (e.g., Armijo et al., 1986; Elliott et al., 2010; Gan et al., 2007; Ge et al., 2015; Li et al., 2020; Molnar and Chen, 1983; Molnar and Lyon-Caen, 1989; Molnar and Tapponnier, 1978; Ni and York, 1978; Shen et al., 2005; Wang et al., 2001; Zhang et al., 2004). Detailed studies of individual grabens throughout Tibet suggest that the widespread normal faulting began since ca. 8–15 Ma (e.g., Blisniuk et al., 2001; Edwards and Harrison, 1997; Garzione et al., 2003; Harrison et al., 1992, 1995; Kali et al., 2010; Lee et al., 2011; McCallister et al., 2014; Murphy et al., 2002; Pan and Kidd 1992; Sanchez et al., 2013; Saylor et al., 2010; Styron et al., 2013; Woodruff et al., 2013).

In the context of active large-scale deformation of eastern Asia, the E-W extension across the Tibetan Plateau is reflected by GPS data showing more rapid eastward movement of eastern than western Tibet relative to the stable Eurasia (see sub-map in Fig. 1). This extension is especially clear when velocities are plotted in a "Tibetan Plateau-fixed" reference frame obtained by minimizing the net movement of sites within the plateau (Gan et al., 2007) (Fig. 1).

East of the highest part of the plateau, GPS velocities show a clockwise rotation and eastward transport of the southeastern plateau, around the Eastern Himalayan Syntaxis (e.g., Gan et al., 2007; Li et al., 2020; Wang et al., 2001; Zhang et al., 2004). The smoothly varying velocity field southeast of Tibet raises the question of when did that pattern of deformation begin and did it occur concurrently with the onset of normal faulting in central and southern Tibet.

To address the timing of clockwise rotation about the eastern syntaxis, we exploit current rates of crustal deformation based on GPS velocities, and we use fault traces as passive markers that are being distorted by that deformation. In particular, we rely on the warping of the Red River fault (Schoenbohm et al., 2006) and the displacement and shear of the Yalong-Yulong thrust belt, which forms the southwestward continuation of the Longmen Shan thrust belt (e.g., Burchfiel and Chen., 2012; Liu-Zeng et al., 2008; Wang et al., 1998; Xu et al., 2003) (Fig. 2). We assume that the current horizontal deformation rate approximates the long-term rate. We contend that both theory and observations justify such extrapolations.

In geodynamics, the equation of equilibrium, or Stokes's equation, balances gradients of components of stress with the body force due to gravity. Forces that induce deformation of parcels of lithosphere are matched exactly by viscous forces that resist deformation, for the acceleration, and therefore the total force at any point, is zero. Consequently, changes in rates of deformation can arise only because of changes in boundary conditions or by alterations of rheological parameters, like viscosity, that relate stress to strain rate. As rheological properties are affected most strongly by temperature, and characteristic time constants for diffusion of heat through the lithosphere are

Weijun Gan  <https://orcid.org/0000-0003-0673-1587>

\*Corresponding author: [wjgan@ies.ac.cn](mailto:wjgan@ies.ac.cn).

<sup>§</sup>peter.molnar@colorado.edu (P. Molnar); [zhangpeizhen@mail.sysu.edu.cn](mailto:zhangpeizhen@mail.sysu.edu.cn), [peizhen@ies.ac.cn](mailto:peizhen@ies.ac.cn) (P. Zhang); [grxiao@ecit.edu.cn](mailto:grxiao@ecit.edu.cn) (G. Xiao); [liangshiming@ies.ac.cn](mailto:liangshiming@ies.ac.cn) (S. Liang); [kzhang@ies.ac.cn](mailto:kzhang@ies.ac.cn) (K. Zhang); [george\\_jun@hotmail.com](mailto:george_jun@hotmail.com) (Z. Li); [12xkk@tongji.edu.cn](mailto:12xkk@tongji.edu.cn) (K. Xu); [zhangling4255@126.com](mailto:zhangling4255@126.com) (L. Zhang).

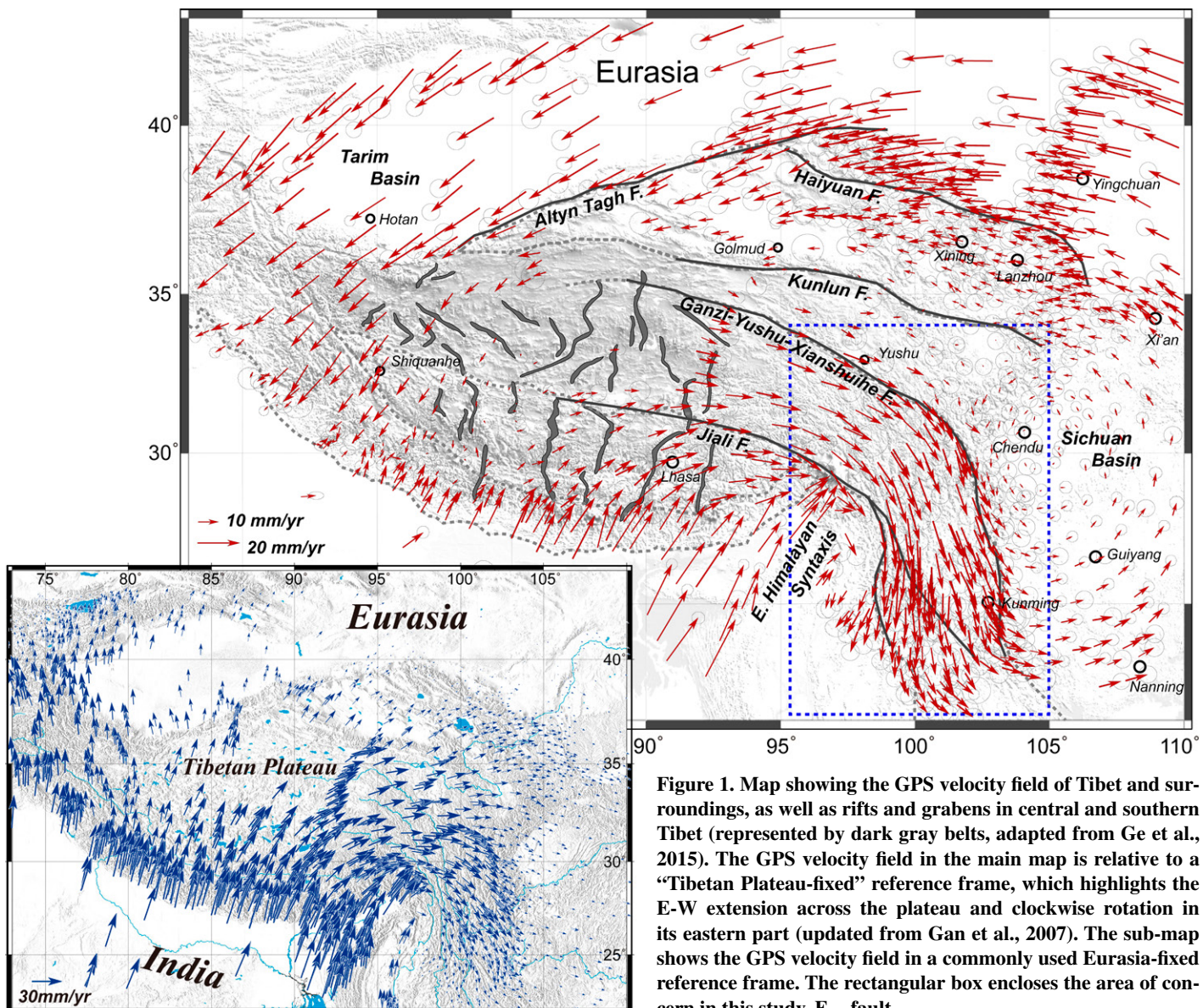


**Figure 1.** Map showing the GPS velocity field of Tibet and surroundings, as well as rifts and grabens in central and southern Tibet (represented by dark gray belts, adapted from Ge et al., 2015). The GPS velocity field in the main map is relative to a “Tibetan Plateau-fixed” reference frame, which highlights the E-W extension across the plateau and clockwise rotation in its eastern part (updated from Gan et al., 2007). The sub-map shows the GPS velocity field in a commonly used Eurasia-fixed reference frame. The rectangular box encloses the area of concern in this study. F.—fault.

tens of millions of years, such changes ought to have little effect on rates of deformation on the million-year time scale. Changes in lateral boundary conditions can occur on shorter time scales, such as when a new plate boundary forms, but such events are rare. For convergence between India and Eurasia, which is directly related to our study area, the rate and direction have changed little since ca. 10 Ma or more (e.g., DeMets et al., 2020; Molnar and Stock, 2009).

Changes in bottom boundaries, such as by the removal of mantle lithosphere, seem also to be possible in the few-million-year time scale (e.g., Bird and Baumgardner, 1981; Houseman et al., 1981), but such events also seem to be rare. Evidence of such a process is sparse, and

we are unaware of evidence suggesting that removal of mantle lithosphere has occurred more than once in the typical tens-of-millions-of-year lifetimes of major mountain belts. Thus, in regions that have undergone deformation for periods as long as tens of millions of years, changes in rates of large-scale deformation that exceed several tens of percent ought to be rare, and occur only once, or at most twice, in such periods.

At the largest scale, numerous studies of high-resolution histories of relative plate motion show only small, <20% changes in relative velocities over ~10 m.y. periods (e.g., DeMets and Merkouriev, 2016; DeMets et al., 2005, 2015a, 2015b, 2020; Iaffaldano, 2014; Iaffaldano et al., 2014; Merkouriev

and DeMets, 2006, 2008, 2014). In a noteworthy exception, convergence between the Nazca and South America plates seems to have changed by ~30% over a few-million-year period (DeMets and Merkouriev, 2019; Garzione et al., 2006; Iaffaldano et al., 2006), when the Central Andes seem to have risen 2–3 km in a comparably short period, and when mantle lithosphere seems to have been removed from beneath the region (e.g., Garzione et al., 2006, 2008; Gubbels et al., 1993; Kennan et al., 1997; Schildgen et al., 2007). The assumption of constant rates of relative plate motion, in fact, enabled Wilson (1993) to test refinements of the geomagnetic time scale, and Krijgsman et al. (1999) to refine that time scale further.

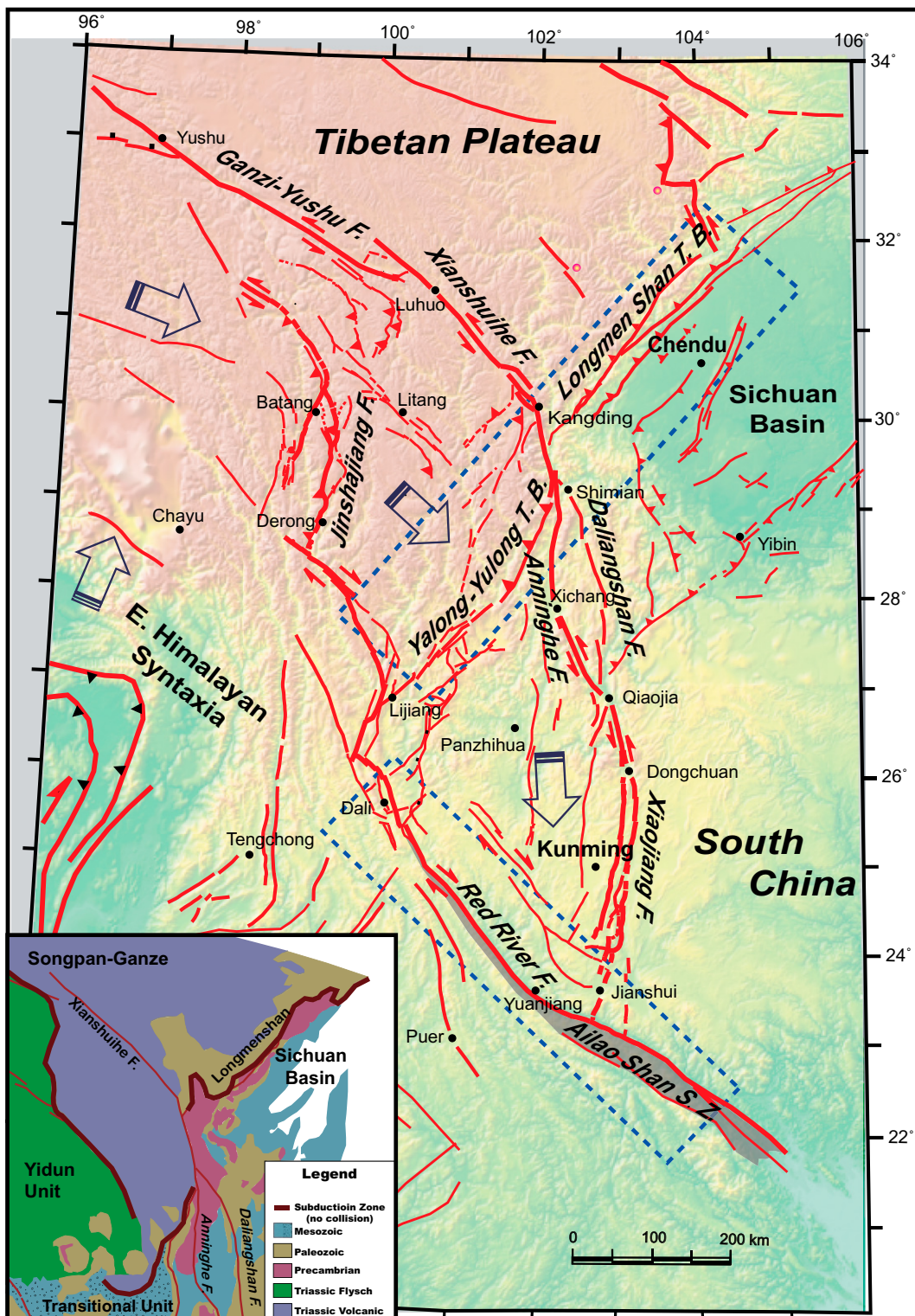


**Figure 2.** Schematic tectonic map showing the major faults around the southeast margin of the Tibetan Plateau (adapted from Xu et al., 2003). The Red River fault (F.) and Yalong-Yulong-Longmen Shan thrust belt (T.B.), framed by the dashed boxes, are the focus of this study. Thick arrows show movement relative to South China. Inset shows an ancient subduction zone, part of which now lies along the Yalong-Yulong-Longmen Shan thrust belt and apparently has been offset by slip on the Xianshuihe fault (adapted from Burchfiel and Chen, 2012). F.—fault; S.Z.—shear zone; T.B.—thrust belt.

We recognize that changes in rates of deformation must necessarily occur to build mountain ranges and high plateaus, but we assume that in periods spanning tens of millions of years, horizontal deformation rates, such as the rotational deformation about the syntaxis, can occur at essentially constant rates over such periods.

#### DEFLECTIONS OF THE RED RIVER FAULT AND YALONG-YULONG-LONGMEN SHAN THRUST BELT

The Ailao Shan shear zone, a long-standing, deeply exhumed fault zone, underwent several hundred kilometers of Oligo-Miocene

left-lateral shear (Harrison et al., 1996; Le-loup et al., 2001; Searle et al., 2010; Tapponnier et al., 1986; Wang and Burchfiel, 1997). Since 10–14 Ma, however, the Red River fault, which follows approximately the northeast margin of the Ailao Shan shear zone (Fig. 2), has undergone right-lateral displacement of 25

TABLE 1. BASIC INFORMATION OF GPS VELOCITY DATA SETS

Data set	Number of stations	Time span	Survey mode	Source
NW Vietnam	19	≤3 years	Campaign mode: 3–8 surveys during 2001–2012	Duong et al. (2013)
N Vietnam	13	≤3 years	Campaign mode: 2–5 surveys during 1994–2007	Tran et al. (2013)
Eastern Himalayan Syntaxis	6	≤6 years	Campaign mode: 7 surveys during 2007–2013	Devachandra et al. (2014)
Bhutan	30	≤11 years	Campaign mode: 3 surveys in 2001, 2003, and 2012	Vernant et al. (2014)
Eastern Himalayan Syntaxis	10	≤8 years	Campaign mode: ≥3 surveys during 2006–2013	Gupta et al. (2015)

km (Replumaz et al., 2001), ~40 km (Schoenbohm et al., 2006), or 20–54 km (Wang et al., 1998). This reversal in regional deformation implies other changes in relative motions of surrounding domains. Important for us here, the Red River fault is not straight, but shows a marked left-lateral deflection of ~60 km across a region 100–200 km in width in the middle segment where the Xianshuihe-Xiaojiang fault approaches it (e.g., Schoenbohm et al., 2006; Wang et al., 1998) (Fig. 2). So, although active as a right-lateral strike-slip fault, the trace of Red River fault serves as a passive marker, deflected by shear of an internally deforming region around the Eastern Himalayan Syntaxis (Schoenbohm et al., 2006).

The Longmen Shan thrust belt lies within the Longmen Shan, the mountain range that separates the eastern Tibetan Plateau from the Sichuan Basin. We do not refer to the active thrust fault at that margin (e.g., Hubbard and Shaw, 2009; Zhang, 2013), but rather to a thrust belt that apparently began to develop in Late Triassic, and that accommodated significant crustal shortening during the Indosinian Orogeny in Mesozoic time (e.g., Burchfiel et al., 1995; Chen and Wilson 1996; Li et al., 2003; Searle et al., 2016; Wallis et al., 2003; Xue et al., 2017; Yan et al., 2011). Most agree with Burchfiel et al. (1995) that much of the crustal thickening in this region occurred in Mesozoic time. The Late Triassic Longmen Shan thrust belt, including deformed and metamorphosed surrounding rock, has been cut and offset ~60 km by the NNW-trending Xianshuihe fault (Burchfiel et al., 1995; Wang et al., 1998; Wang et al., 2009) (Fig. 2). As shown by Liu-Zeng et al. (2008) and Xu et al. (2003), the southwestward continuation of the Longmen Shan thrust belt, the Yalong-Yulong thrust belt, has been displaced ~100 km by southeastward crustal extrusion, and forms an arcuate trace with a length of ~200 km (Fig. 2).

As both the Red River fault and the Yalong-Yulong-Longmen Shan thrust belt existed before the late Miocene, their fault traces form regional strain markers of the southeastern plateau margin that have been deflected. Their deflections record shear that has accumulated by clockwise rotation that initiated since those features formed. We can estimate the date of the initiation of clockwise rotation by retro-deforming the deflected fault

traces using current deformation rates from GPS velocities, and assuming that their original shapes of the traces were overall straight.

### GPS VELOCITIES

About 85% of the GPS velocities in Figure 1 are from published solutions of two Chinese national scientific projects, Crustal Movement Observation Network of China (CMONOC-I) and Tectonic and Environmental Observation Network of Mainland China (CMONOC-II) (Li et al., 2012). The detailed GPS observation methods and data processing strategies were introduced by Gan et al. (2007) and Liang et al. (2013). In addition to the GPS velocity data set of 423 stations from CMONOC, we merged some other published GPS velocities (Table 1) to enhance the density and coverage of GPS stations.

Although the CMONOC velocities and those of other data sets commonly are given in Eurasia-fixed reference frames, those frames differ slightly from each other. As each of the other data sets shared some stations with the CMONOC data set, we used stations common to the CMONOC data set as “links” to transform all the other velocities into the same reference frame as that for CMONOC by using rigid-body rotations with appropriate angular velocities. After the reference frame transformations, the maximum differences of north and east components of the velocities for the same stations in different data sets are 2.1 and 1.6 mm/yr, respectively; these values are within two standard deviations of the velocity components. The final velocities of the common stations are the weighted average of the values from all the data sets in the same Eurasia-fixed reference frame.

Two major earthquakes, 2008 Wenchuan Mw 7.9 (e.g., Zhang, 2013; Zhang et al., 2010) and 2013 Lu Shan Ms 7.0 earthquakes (Xu et al., 2013), occurred in the area of this study during the GPS observation span. In order to avoid the contamination by transient displacements associated with these two events, we excluded the GPS data observed after the earthquakes for those stations located within ~500 km of the epicentral areas of those earthquakes.

The combined velocities of 501 GPS stations in the Eurasia-fixed reference frame demon-

strate the well-known crustal movement pattern (see sub-map in Fig. 1), but to highlight the clockwise rotation around the southeastern plateau margin relative to its stable neighbor block to the east, we transformed the velocities into a reference frame fixed to the South China Block, by minimizing the root mean square velocities of 83 stations located in that block (Fig. 3A). Not only is the rotation about the syntaxis clear, but it also is confined to the region west of the South China Block bounded by the Xianshuihe-Xiaojiang fault zone on the north and east, and therefore includes a major component of left-lateral shear along that boundary (Figs. 2 and 3A).

### ESTIMATION OF INITIATION AGE

The surface traces of the Red River fault and Yalong-Yulong-Longmen Shan thrust belt (hereafter “fault traces”) are deflected left-laterally by the clockwise rotation around the eastern syntaxis. Moreover, marked gradients in GPS velocities characterize the segments of the fault traces where they are deflected. In order to estimate the initiation age of the clockwise rotation and the deflections of the fault traces using GPS velocity field, we adopted the following strategy:

(1) By extending the undeflected segments of the fault traces, we defined two directions, N138°E and N51°E, which are approximately parallel to the traces in the regions where present-day rotation is modest (Fig. 3A).

(2) The exact positions of the initial fault traces are unknown, but they can be represented approximately by linear extensions of the undeflected segments. By representing the current fault traces as a series of points, we further defined a series of expected corresponding points on the extensions of the undeflected segments (Fig. 3B). Using the positions of these points, we first obtained appropriate velocities of these points (shown as the blue vectors in Fig. 3B) by interpolation from the GPS velocity field using the interpolation algorithm of splines in tension ( $\tau = 0.95$ ) (Wessel and Bercovici, 1998; Gan et al., 2007). We then averaged the velocities of each pair of corresponding points. The averaged velocities (shown as the red vectors in Fig. 3B) were appointed to represent the long-term velocities of the fault traces.

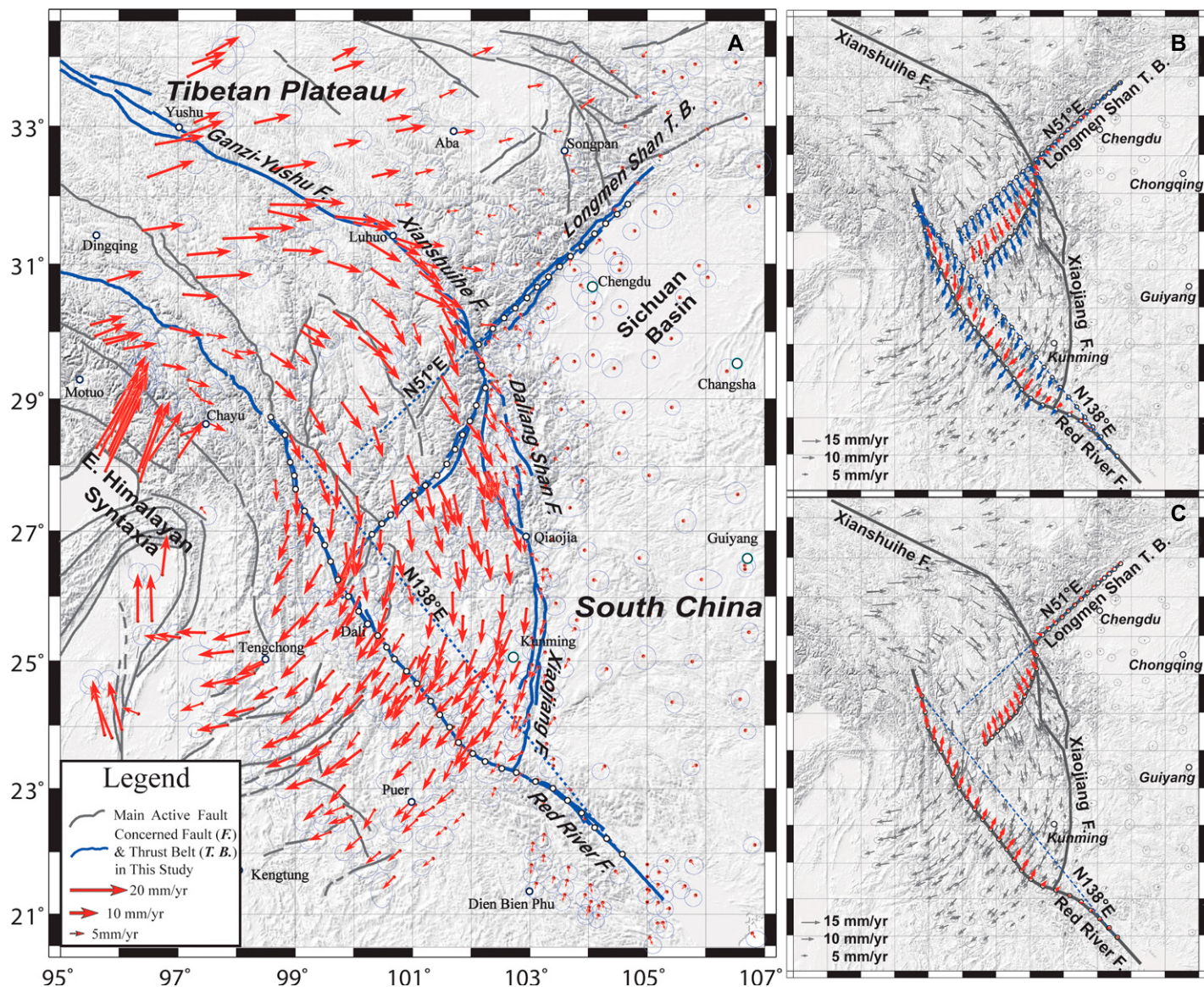


**Figure 3.** (A) Map showing the GPS velocity field relative to the stable South China Block (with error ellipses of 95% confidence). Continuations of the Red River fault (F.) and Yalong-Yulong-Longmen Shan thrust belt (T.B.) traces are represented by beaded lines. The thin dashed lines directed toward N138°E and N51°E mark extensions of non-deflected segments of the two faults. (B) The blue arrows show velocities at points on fault traces and dashed lines and are interpolated from the background GPS velocities, and the red arrows show averages of corresponding blue arrows. (C) Map showing our strategy to estimate ages when bending of the faults began by letting the points on the current fault traces move backward with the average velocities (the red arrows) until they recover shapes that are closest to straight lines.

(3) We assume that all points on the original fault traces have moved with current average velocities since the traces were deflected. We assume that the initial shapes of the fault traces were straight, and we let points on the current fault traces move backward (Fig. 3C) until they recover a shape that is closest to a straight line (Fig. 4).

With the above strategy, we estimated similar ages of initiation of 9.6 Ma and 10.7 Ma from the Red River fault and Yalong-Yulong-

Longmen Shan thrust belt, respectively, and therefore 10.1 Ma.

As we know, the overall shape of the initial fault trace need not be straight, although in theory and practice, it is more common for thrust and strike-slip faults to evolve into overall linear features. Hence, the estimation based on the ideal linear assumption could include deviations, which sometimes are not insignificant. We estimated the  $1\sigma$  uncertainty of the initiation age with two approaches. First,

the two independently deduced initiation ages were quite consistent, with a difference of  $\sim 1.1$  m.y., which provided us with some clues to assess the level of uncertainty. Second, we empirically assumed that the best fitting line is not significantly different from the other good fitting lines when differences in correlation coefficients between them are less than  $\sim 1\%$  of the correlation coefficient difference between the current and original fault traces in the inversion by least-squares linear fitting

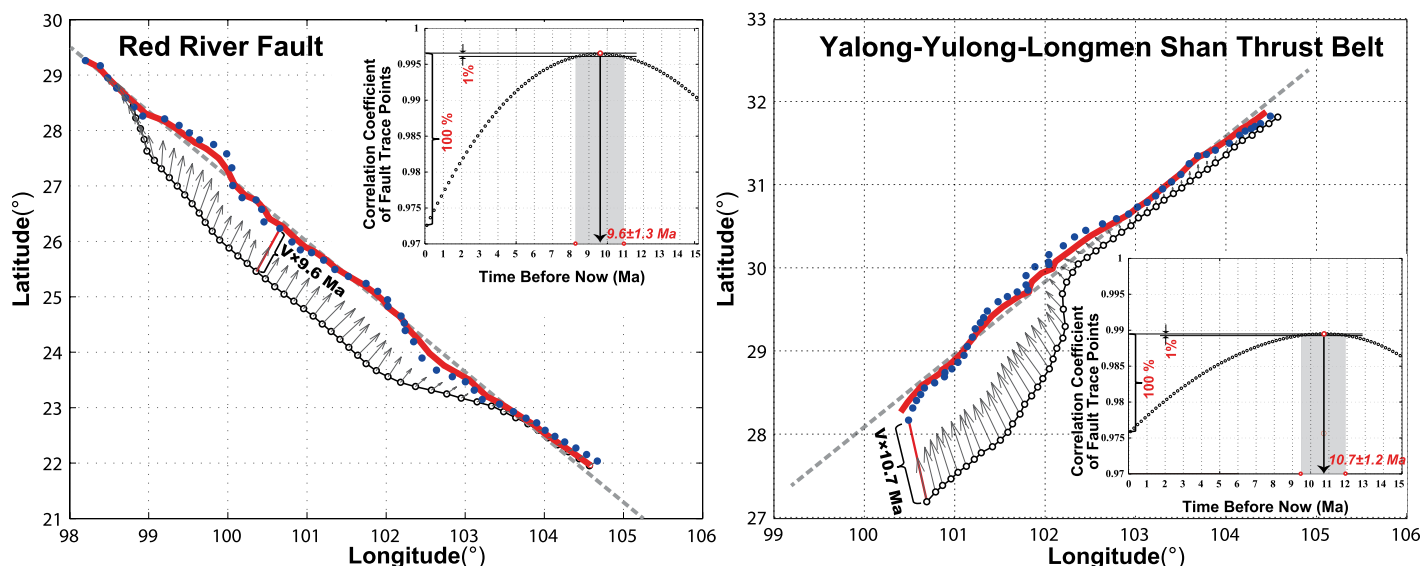


**Figure 4.** Schematic map showing the predicted original fault traces (thick red lines) of the Red River fault and Yalong-Yulong-Longmen Shan thrust belt, along the southeast margin of the Tibetan Plateau, with initiation ages of  $9.6 \pm 1.3$  Ma and  $10.7 \pm 1.2$  Ma, respectively. The blue dots show predicted original positions of the corresponding black circles on current fault trace using the velocities (gray arrows) and the best estimate of initiation age. The thick red lines are smoothed out by averaging the predicted fault trace points (blue dots) and corresponding best fitting straight lines (gray dash line), so as to better represent the original fault traces without jagged edges. Each inset shows the correlation coefficient of weighted linear fitting of the points predicted by different duration times has a unique maximum, which corresponds to the best fit to a straight line and thus the best estimate of the initiation age. The  $1\sigma$  uncertainties of ages are empirically determined based on the assumption that the best fitting line is not significantly different from the other good fitting lines when the difference of correlation coefficient between them is less than ~1% of the correlation coefficient difference between the current and original fault traces. Thus, we determine the ranges of the best-fitting age (gray boxes), and in turn, determine the uncertainty of the ages.

(see sub-maps in Fig. 4). This approach yielded  $1\sigma$  uncertainties of  $\pm 1.3$  Ma and  $\pm 1.2$  Ma for the Red River fault and Yalong-Yulong-Longmen Shan thrust belt, respectively. Based on the above empirical assessment, we set  $\pm 1.5$  Ma as a conservative estimate of the  $1\sigma$  uncertainty, and therefore  $10.1 \pm 1.5$  Ma for the estimate of initiation age. Obviously, readers could multiply this uncertainty by a factor greater than one, if they doubted the approach. It should also be noted that the estimate in our method is affected mainly by the overall linearity of the fault traces, and not the local twists and turns in the traces. Figure 4 shows that the inferred original fault traces locally twist and turn and do not form ideal straight lines.

## DISCUSSION

### Comparison of Palaeomagnetic Declination Anomalies with GPS Observed Rotations

Numerous paleomagnetic studies show clockwise declination anomalies of rock from eastern Tibet, including the region northeast of the syntaxis to western Yunnan, southeast of Tibet. Thus, they indicate clockwise rotation of

such rock. Two processes have contributed to these rotations. First, the present-day GPS velocity field (Fig. 3A) includes rotation about a vertical axis. The current pattern of flow around the eastern syntaxis includes clockwise rotation, but the amount is small. For a maximum rate of  $\sim 10$  mm/yr about the syntaxis and  $\sim 500$  km from it, displacement of  $\sim 100$  km since 10 Ma, yields a rotation of only  $\arctan(100/500) \approx 11^\circ$ . Second, and more importantly, as India penetrated into Eurasia, both it and the region to its north moved northward with respect to South China, and induced right-lateral shear and clockwise rotation of eastern Tibet (e.g., Cobbold and Davy, 1988; Davy and Cobbold, 1988; England and Molnar, 1990; England and Houseman, 1986). Blocks embedded in a zone of simple shear of width,  $L$ , and across which opposite sides are displaced  $\Delta u$  should undergo rotation,  $R$ , such that  $\arctan(\Delta u/2L) < R < \arctan(\Delta u/L)$ , that is dependent on the shape of the object and boundary conditions (Lamb, 1987; McKenzie and Jackson, 1983). With a width  $L \approx 500$  km for eastern Tibet, and values of  $\Delta u$  between 200 km in the north and 1000 km in the south, we might expect  $R \sim 10^\circ$ – $25^\circ$  in the north and  $R \sim 45^\circ$ – $65^\circ$  in the south. Although

the contributions of both processes to clockwise rotation are apparent, separating them is tricky, and the role of the first of these processes cannot be assessed well.

Despite scatter, amounts of clockwise rotation inferred from paleomagnetic declinations increase southward, as expected. In the northern region near latitudes of  $\sim 35^\circ$ , where though present-day left-lateral slip on east-west planes and therefore counterclockwise rotation characterizes current deformation (Duvall and Clark, 2010), total amounts of clockwise rotation are  $\sim 15^\circ$ – $25^\circ$  (Dupont-Nivet et al., 2004, 2008; Fang et al., 2003; Liu et al., 2010; Wang et al., 2011; Yan et al., 2006). Near the latitude of the syntaxis, most estimates of clockwise rotation are  $25^\circ$ – $50^\circ$  (e.g., Huang et al., 1992; Kornfeld et al., 2014; Otofuji et al., 1990; Todrani et al., 2020; Zhang et al., 2020). Farther south in Yunnan, yet larger amounts of clockwise rotation exceeding  $50^\circ$  (Chen et al., 1995; Huang and Opdyke, 1993; Li et al., 2018; Tong et al., 2016) and reaching  $90^\circ$  (Sato et al., 2001) have been reported, but many sites show smaller amounts of rotation. As important as the southward increase in amounts of rotation is the scatter in such data. In a particularly thor-

ough study of the region just south of the Litang fault (Fig. 2), Todrani et al. (2020) reported a range from  $26^\circ \pm 12^\circ$  of counterclockwise rotation to as much as  $37^\circ \pm 8^\circ$  clockwise rotation, with three sites with as much as  $60^\circ$  to  $86^\circ$  clockwise rotations. Similarly, although large rotations have been recorded from parts of Yunnan, smaller amounts have also been measured:  $36.3^\circ \pm 13.6^\circ$  (Sato et al., 1999),  $26^\circ \pm 17^\circ$  (Funahara et al., 1992),  $25^\circ \pm 16^\circ$  (Funahara et al., 1993),  $12.1^\circ \pm 10.0^\circ$  (Otofuji et al., 1998),  $\sim 4^\circ \pm 8^\circ$  (Yoshioka et al., 2003), essentially no rotation at a site next to the Red River fault (Huang and Opdyke, 1993) and even counterclockwise  $8^\circ \pm 3^\circ$  (Li et al., 2015) albeit from a site near the Xiaojiang fault. These rotations are given relative to Eurasia, but a better reference frame might be South China. Although paleomagnetic studies of its western edge show essentially no rotation (e.g., Huang and Opdyke, 1992; Otofuji et al., 1990), several sites surrounding the Sichuan Basin suggest a small clockwise rotation of  $5\text{--}10^\circ$  (Tong et al., 2020). Thus, values given above might be reduced by that amount.

As noted above, the current pattern of flow around the syntaxis contributes to the clockwise rotation but the estimated amount of  $\sim 11^\circ$  is small compared with paleomagnetic declination anomalies. Moreover, most of the largest values ( $50^\circ\text{--}90^\circ$ ) come from south of the region currently undergoing that rotation around the syntaxis. Otofuji et al. (2010) suggested that these regions with large paleomagnetic declinations underwent rotation when they lay near the eastern syntaxis, and subsequently were displaced southeastward, where GPS data show that only slow rotation occurs today. In a review of paleomagnetic data from Yunnan and surrounding regions, Tong et al. (2021) concluded that rotation began since ca.  $25.7 \pm 2.5$  Ma at a higher rate than occurs today, despite scatter in amounts of rotation. At that time, the syntaxis would have lain  $\sim 1000\text{--}1500$  km south of its current position with respect to South China, and hence west of this region where large rotations have accumulated. We conclude that the paleomagnetic declinations, despite scatter, have resulted largely from right-lateral shear of eastern Tibet and not from the ongoing flow around the syntaxis.

#### Approximate Synchronization with a Suite of Tectonic Deformation Events

The estimated initiation age,  $10.1 \pm 1.5$  Ma, of clockwise rotation of the southeastern plateau margin is approximately synchronous with a suite of tectonic phenomena, both near and far, within the scope of the wide Eurasia/Indian col-

lision zone (Fig. 5), which collectively indicate that a major tectonic event happened since the middle Miocene.

#### Onset of the Ganzi-Yushu-Xianshuihe Fault

The region undergoing clockwise rotation around the Eastern Himalayan Syntaxis is bounded on the north by the Ganzi-Yushu-Xianshuihe fault, which crops out as a ductile shear zone that consists of mylonite with mylonitized and migmatitized rock (Xu et al., 2007; Wang et al., 1998) (Fig. 2). The Xianshuihe segment offsets a huge Precambrian metamorphic complex left-laterally for 90–100 km. Also, a granodiorite body, with a length parallel to the Xianshuihe fault for 80–90 km and a width of only 7–20 km, was emplaced along the fault near the offset of the belt (Xu et al., 2007). From micro-structure and geochemical studies, Xu et al. (2007) suggested that this linear granodiorite was emplaced during the initiation of left-lateral displacement on the Xianshuihe fault, and thus, the age of emplacement dates the onset of slip on the fault. Roger et al. (1995) obtained U-Th and Rb-Sr ages of 10–12 Ma, and Xu et al. (2007) reported a Rb-Sr age of  $9.9\text{--}11.6$  Ma, which are consistent with the inference that clockwise rotation began at  $10.1 \pm 1.5$  Ma, though Searle et al. (2016) suggested that slip might have begun at only 5 Ma.

Along the whole Ganzi-Yushu-Xianshuihe fault zone, the Ganzi-Yushu segment has the simplest geometrical structure (Fig. 2). Field investigations show that this segment has a total left-lateral offset of 75–80 km based on a dislocated Triassic granitic pluton (Wang et al., 1998). Wang et al. (2009) claimed that fission track ages decreased toward the fault zone, and they assumed that the oldest ( $12.8 \pm 1.4$  Ma) marked the date when the fault became active. In fact, by relying on GPS velocities, inferred late Quaternary offsets of moraines and other features, and a total offset of precisely dated igneous rock, Chevalier et al. (2017) inferred that the slip rate on the Ganzi-Xianshuihe fault (Fig. 1) has been constant since slip began at, or shortly after, ca. 12.6 Ma. Thus, one could derive a long-term average slip rate of 5.9–6.3 mm/yr based on the date and total offset. Multiple estimates of short-term average slip rates for late Quaternary or Holocene periods from the classic methods of dating offset landforms like terraces and alluvial fans have yielded a slip rate of  $\sim 7$  mm/yr (Chevalier et al., 2017; Li et al., 1995; Zhou et al., 1996). In addition, GPS observations give a present-day slip rate of  $6.6 \pm 1.5$  mm/yr (Wang et al., 2013). If the slip rate had been constant at 6.6 or 7.0 mm/yr, then 75–80 km of offset would imply an onset date of 10.7–12.1 Ma for the Ganzi segment.

Thus, these onset dates of the Ganzi-Yushu-Xianshuihe fault are indistinguishable from  $10.1 \pm 1.5$  Ma, and the fault became active synchronously with the eastward transport and clockwise rotation.

#### Slip Reversal of the Red River Fault

The Red River fault is a first-order tectonic structure in the southeast margin of the Tibetan Plateau; it separates the South China Block to the northeast and the Indochina block to the southwest (Fig. 2). Numerous studies determined that the Red River fault experienced a reversal of slip from left- to right-lateral sometime between 16 Ma and 5.5 Ma (Allen et al., 1984; Wang et al., 1998; Replumaz et al., 2001; Schoenbohm et al., 2006; Zhu et al., 2009). Recently, based on the seismic analysis and stratigraphic information from confidential exploration wells in the Gulf of Tonkin, where the offshore segment of the Red River fault lies, Fyhn and Phach (2015) suggested that the reversal of slip may have commenced at ca. 10–8 Ma. In addition, Wang et al. (2016), using new apatite (U-Th)/He data together with existing thermochronological data, backed by stratigraphic, structural, and geomorphologic observations, inferred that the Ailao Shan-Red River shear zone experienced a phase of rapid cooling and exhumation starting near 14–10 Ma, and then, since 10 Ma a reversal from left-lateral slip on the Ailao Shan shear zone to right-lateral slip on the Red River fault. Again, these tectonic phenomena coincide with our estimate of the initiation of clockwise rotation of the southeastern Tibet.

#### Rapid River Incision Due to Rapid Increase in Mean Elevations of Southeast Tibet

In eastern Tibet east of the eastern syntaxis of the Himalaya, age-elevation transects of low-temperature thermochronometers suggest slow cooling between 100 Ma and 10–20 Ma and a change to rapid river incision between ca. 8 Ma and 13 Ma (Clark et al., 2005; Godard et al., 2009, 2010; Ouimet et al., 2010; Zhang et al., 2016). Thus, these data can be interpreted to indicate surface uplift, presumably in response to crustal thickening, concurrent with the onset of rotation in this region.

#### Deformation within the Tibetan Plateau

Since the initial recognition of active N-S-trending rifts in southern Tibet (Armijo et al., 1986; Molnar and Tapponnier, 1978; Ni and York, 1978; Tapponnier and Molnar, 1977), numerous studies have constrained the timing of the rift-related normal faulting and E-W crustal extension, as the onset of extension was argued to represent the time when the plateau began to collapse after it reached its highest elevation (England and Houseman 1989; Harrison et al., 1992; Molnar

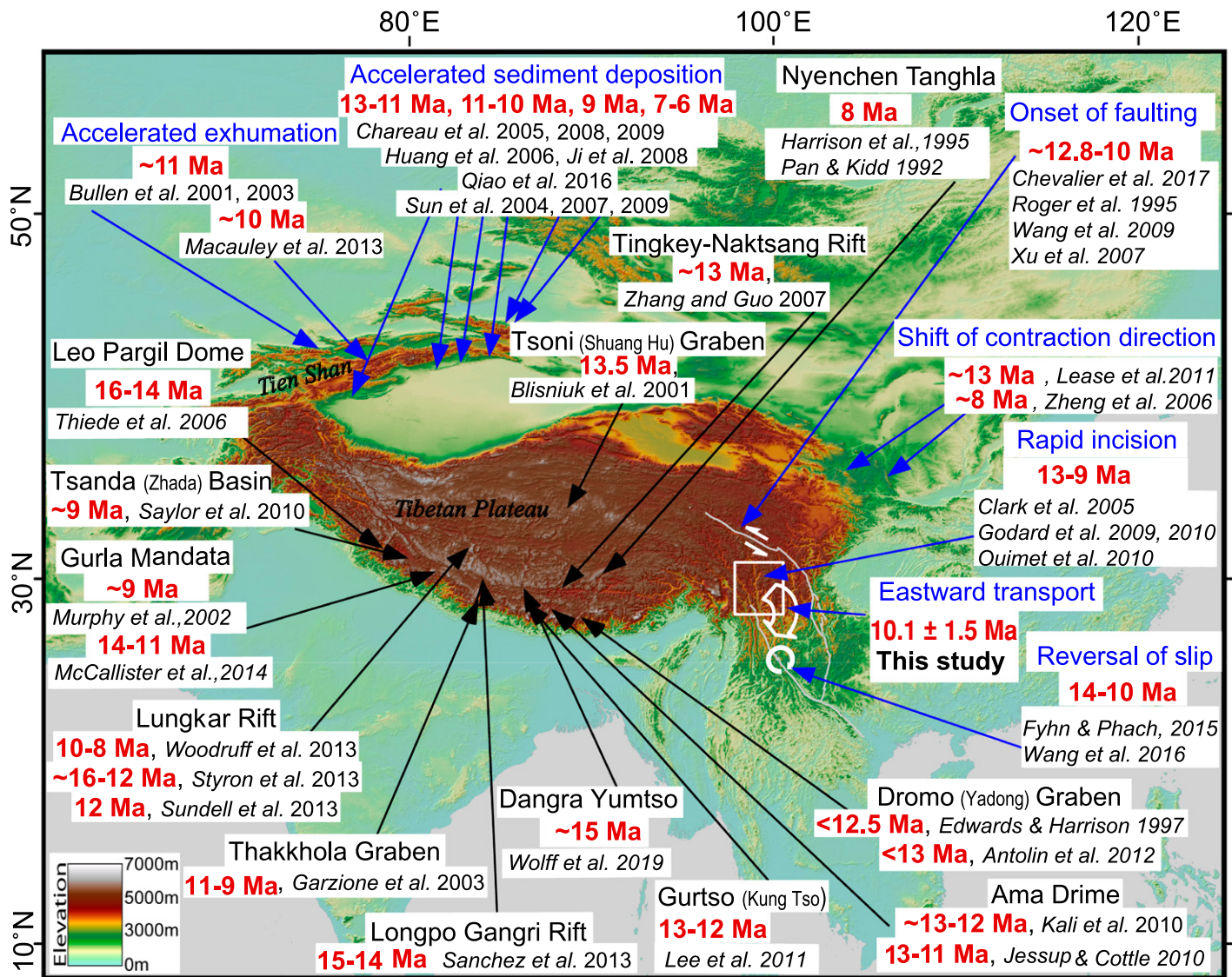


**Figure 5.** Distribution of the tectonic events that occurred within and around the Tibetan Plateau near 10–15 Ma. The black arrows point to locations of normal faulting in the plateau interior. The blue arrows point to the locations of other tectonic events marked by blue text.

et al., 1993). Reported dates of onsets of normal faulting and crustal thinning range from 15 Ma to 8 Ma (e.g., Blisniuk et al., 2001; Dewane et al., 2006; Edwards and Harrison, 1997; Garzione et al., 2003; Kali et al., 2010; Lee et al., 2011; McCallister et al., 2014; Murphy et al., 2002; Sanchez et al., 2013; Saylor et al., 2010; Thiede et al., 2006; Wu et al., 2008) (Fig. 5). The relatively wide spread of ages, and the apparent absence of strict simultaneity with the onset of rotation about the eastern syntaxis may be due in part to inaccuracies in ages. More important, however, if development of normal faulting and crustal thinning did result from removal of mantle lithosphere, we would not expect such a process to have occurred

at the same time across the whole of Tibet. Moreover, only after the entire plateau was undergoing extension and crustal thinning, would the effects of its increase in gravitational potential energy affect surrounding regions.

#### Deformation of Regions North and Northeast of Tibet

In northeastern Tibet, early Cenozoic deformation was accommodated primarily by slip on WNW-trending thrust faults, which indicates that during the early stages of orogenesis, the orientation of thrust faulting was approximately parallel to the orientation of plate convergence. Nevertheless, some studies reveal a middle-

late Miocene change in the kinematic style of plateau growth, from long-standing NNE-SSW contraction that mimicked the orientation of plate convergence to the initiation of new structures accommodating E-W contraction (e.g., Lease et al., 2011; Zheng et al., 2006). Lease et al. (2011) reported apatite (U-Th)/He and apatite fission track ages from Laji-Jishi Shan in the northeastern Tibetan Plateau (Fig. 5), from which they inferred that accelerated growth of the WNW-trending eastern Laji Shan began ca. 22 Ma. Rapid growth of the adjacent, but north-trending Jishi Shan, however, did not commence until ca. 13 Ma. Thus, the primary orientation of contraction in the

composite Laji-Jishi Shan changed  $>45^\circ$  with the initiation of E-W shortening of the Jishi Shan. Furthermore, paleoclimate records from sediment in Neogene basins on either side of the Jishi Shan show the development of a rain shadow due to surface uplift of the range by ca. 11 Ma, but not before ca. 16 Ma (Hough et al., 2011). Zheng et al. (2006), using apatite fission track thermochronology, found that late Cenozoic rapid cooling occurred at ca. 8 Ma in the Liupan Shan region (Fig. 5), and the north-trending thrust faults there began to accommodate lateral motion at that time. This inception of E-W contraction is only slightly later than the eastward transport and clockwise rotation in southeastern Tibet, and reflects a change in the kinematic style of plateau uplift and lateral growth. Lateral, outward growth of the margin of the plateau should begin later than crustal shortening that is now within the high terrain.

North of the Tibetan Plateau, the current rate of convergence across the western Tien Shan is  $20 \pm 2$  mm/yr (Zubovich et al., 2010) and the estimated shortening across the belt is  $\sim 200$  km (Avouac et al., 1993). Assuming a 20% error in the amount of shortening and a constant convergence rate suggests an initiation of crustal shortening at  $10 \pm 2$  Ma (e.g., Abdurakhmatov et al., 1996; Zubovich et al., 2010). Numerous studies of thermochronology, which date the onset of rapid cooling (Bullen et al., 2001, 2003; Macaulay et al., 2013), and of magnetostratigraphy, which date abrupt increases in sedimentation within a few millions years of 10 Ma (Charreau et al., 2005, 2008, 2009; Huang et al., 2006, 2010; Ji et al., 2008; Qiao et al., 2016; Sun et al., 2004, 2009), concur with an abrupt increase in the erosion rate of the Tien Shan, presumably associated with rapid surface uplift, at ca. 10 Ma, though abundant evidence suggests that some relief existed well before ca. 10 Ma.

### Geodynamic Implications of the Approximately Synchronous Reorganization of Deformation

For continental dynamics on a scale in which deformation is averaged over distances comparable to the thickness of the lithosphere, a thin viscous sheet provides a good model (e.g., Bird and Piper, 1980; England and McKenzie, 1982, 1983; Houseman and England, 1986). In this formulation, deformation is resisted both by dissipative, or viscous process, and by gravity where crust thickens. Allowing for strain rates,  $\dot{\epsilon}$ , to vary with deviatoric stress,  $\tau$ , as  $\tau^n$ , the constitutive law can be written:

$$\tau_{ij} = B\dot{E}^{(1/n-1)}\dot{\epsilon}_{ij} \quad (1)$$

where  $B$  is a viscosity coefficient, and  $\dot{E}$  is the second invariant of the strain-rate tensor. Only two dimensionless numbers together with boundary conditions govern solutions to the governing equations,  $n$  ( $\geq 3$ : Sonder and England, 1986) and the Argand number,  $Ar$ :

$$Ar = \frac{g\rho_c L(1 - \rho_c/\rho_m)}{B(V/L)^{1/n}} \quad (2)$$

where  $g$  is gravity,  $\rho_c$  and  $\rho_m$  are the densities of crust and mantle, respectively,  $L$  is the thickness of the thin viscous sheet, and therefore the lithosphere, and  $V$  is a characteristic horizontal component of velocity, like the rate at which the sheet is indented (England and McKenzie, 1982). One may think of  $Ar$  as scaling resistance to crustal thickening imposed by gravity to resistance by viscous processes; if  $Ar \rightarrow 0$ , gravity offers little resistance to crustal thickening, and the sheet is relatively strong, whereas when  $Ar$  is large, crust cannot thicken much because it tends to flow away from regions of thickened crust. The Argand number is sometimes called the fetabrie number, for feta cheese corresponds to small  $Ar$ , and brie to large  $Ar$ .

The reliance on just two dimensionless numbers allows their ranges of values to be explored, and for their roles in large scale deformation to be revealed and assessed (e.g., England and Houseman, 1986; Houseman and England, 1986). Comparisons of large-scale deformation from essentially all regions of large-scale deformation show patterns of deformation that can be matched by treating the continental lithosphere as a thin viscous sheet: eastern Asia (England and Houseman, 1986; England and Molnar, 1997; Flesch et al., 2001; Holt and Haines, 1993; Holt et al., 1991); Iran (Walters et al., 2017); Anatolia (England et al., 2016), and western North America (Bahadori et al., 2018; Flesch et al., 2000; Reitman and Molnar, 2021; Whitehouse et al., 2005). Moreover, strain-rate fields measured at the surface using GPS match those implied by seismic anisotropy in the underlying mantle, which suggests vertically coherent deformation through the lithosphere (e.g., Chang et al., 2015; Davis et al., 1997; Flesch et al., 2005; Holt, 2000).

The simplicity of the thin viscous sheet as a model for continental deformation allows it to reveal how changes in basic conditions or boundary conditions affect deformation. For example, as England and Houseman (1989) argued, a decrease in  $V$ , such as in the rate of indentation of a rigid object, like India, into a thin viscous sheet like the rest of Eurasia, would manifest itself as an increase in  $Ar$ , and hence could affect the pattern of deformation. Because of  $1/n^{\text{th}}$  power of  $V$  in the denominator of  $Ar$ ,

however, a major effect in the deformation field requires a huge change in  $V$ . A change in the viscosity coefficient,  $B$ , should have a bigger effect than comparable change in  $V$ , but insofar as diffusion of heat has the primary effect on viscosity coefficient, such changes will require tens of millions of years to have an effect. Moreover, a concurrent change in  $B$  over an area the size of eastern Asia is implausible.

Both  $n$  and  $Ar$  are material parameters of the thin viscous sheet, and therefore changes in them, such as by changing the thickness of the lithosphere,  $L$ , or its average viscosity coefficient,  $B$ , strictly apply to the entire sheet, so that, in general, the equations solved do not depend separately on the ingredients of  $Ar$  in Equation (2). Lateral variations in  $Ar$ , however, offer the possibility of including more realistic models with the inevitable trade-offs with non-uniqueness and potential loss of simple understanding (e.g., England and Molnar, 1997; Flesch et al., 2001). As England and Houseman (1989) showed, the simplest process that could affect the pattern of deformation in a thin viscous sheet like the eastern Asian lithosphere and give rise to crustal thinning within the Tibetan Plateau would be to raise the surface of the plateau. Doing so would give the elevated region additional gravitational potential energy, which England and Houseman (1989) implemented by *locally* increasing  $Ar$ . They showed that other possible processes, like weakening the part of the sheet occupied by the plateau would have an opposite effect to what is observed. Where weaker, the sheet would shorten and thicken, rather than extend. They argued, and in our view convincingly, that the only way to induce a switch from thickening to thinning would be to raise the surface, and give the plateau additional gravitational potential energy, and greater outward force-per unit length from the plateau. We recognize that others have offered different explanations for the flow of material around the syntaxis, including channel flow within the crust (e.g., Clark and Royden, 2000; Royden et al., 1997; Schoenbohm et al., 2006) and gravity currents (Copley and McKenzie, 2007), and that some question the removal of mantle lithosphere beneath Tibet (e.g., McKenzie and Priestley, 2008). Nevertheless, we consider removal of mantle lithosphere to be the simplest process that can accomplish this increase in gravitational potential energy and the change in tectonic style.

### CONCLUSIONS

The traces of two major fault systems in southwest China, the Red River fault and Yalong-Yulong-Longmen Shan thrust belt, are

currently being distorted by crustal movements in the area southeast of the Tibetan Plateau. GPS measurements show that region currently undergoes widespread, apparently continuous deformation dominated by virtually concentric clockwise rotation about the Eastern Himalaya Syntaxis and associated left-lateral shear of the region (Figs. 1 and 3). By treating current rates of crustal deformation as approximating long-term average rates, we use that velocity field to restore offsets of these fault traces, and suggest that such rotation and shear initiated at  $10.1 \pm 1.5$  Ma.

Significant change in styles and rates of deformation elsewhere in Tibet and its surroundings occurred at approximately the same time. For example, slip on the Ganzi-Yushu-Xianshuhe fault in eastern Tibet apparently began at that time. Slip on the Red River fault seems to have reversed, from left- to right-lateral, at that time. Several rivers began to incise rapidly into southeastern Tibet between 9 Ma and 13 Ma, presumably in response to a rapid increase in mean elevations of that region. Thus, the eastward transport and clockwise rotation seems to be one of several changes in style of deformation across the region.

Approximately concurrently with these changes in eastern Tibet, between 8 Ma and 15 Ma N-S-trending rifts within the Tibetan Plateau, on which E-W extension occurs by normal faulting, developed (Fig. 5). The change from roughly N-S crustal shortening and thickening within the plateau to extension and crustal thinning is arguably the biggest change in style of deformation of Asia since India collided with Eurasia. Also, between 8 Ma and 15 Ma, the orientation of contraction in northeastern Tibet changed from NE-SW—approximately parallel to convergence between India and Eurasia—to E-W, which is perpendicular to the local orientation of the margin of the plateau. Moreover, erosion of the Tien Shan north of Tibet accelerated near 10 Ma, again presumably in response to accelerations of N-S crustal shortening and crustal thickening and the resulting surface uplift (Fig. 5). All of these changes can be seen as a logical response to an abrupt rise of the interior of the Tibetan Plateau at 10–15 Ma. Following England and Houseman's (1989) logic, we concur that mantle lithosphere was removed from beneath the plateau, the surface rose, and the plateau gained gravitational potential energy per unit area. Hence, the elevated plateau applied an increased horizontal compressive force per unit length to its surroundings. The increased gravitational potential energy of that newly elevated terrain then powered outward growth of it, including extension and crustal thinning within the elevated region and en-

hanced crustal thickening of the surrounding regions, including regions as far away as the Tien Shan. The eastward movement of eastern Tibet and the clockwise rotation of that material around the Eastern Himalayan Syntaxis would be local manifestations of this larger geodynamic event. Of course, the surface across a region more than 1000 km in dimension is not likely to have risen simultaneous, let alone instantaneously. Thus, the difference between surrounding regions undergoing a change in tectonic style and rate at ca. 10 Ma, and normal faulting scattered across Tibet starting between ca. 16 Ma and 8 Ma ought not to be a surprise. Convective removal of some or all of Tibet's mantle lithosphere offers the simplest underlying mechanism not just for causing normal faulting within the Tibetan Plateau, but also for affecting the surrounding areas as described above.

#### ACKNOWLEDGMENTS

We thank all the Chinese colleagues who worked in the Crustal Movement Observation Network of China project and collected the GPS data used in this study. We are grateful to Roger Bilham, Huiping Zhang, and two anonymous reviewers for their thoughtful comments, which resulted in considerable improvement of this manuscript. The main figures in the manuscript were drawn with the help of the Generic Mapping Tools. This work was supported by the National Natural Science Foundation of China (41490615), the Special Research Project for Earthquake Science of China (2015419024), and the National Key Research and Development Plan of China (2018YFC1503304).

#### DATA AVAILABILITY STATEMENT

The GPS velocity data set and the solution from this study, which are listed in Tables S2 and S8 of the supporting information<sup>1</sup>, are under way to archive in the Data Sharing Infrastructure of Earth System Science (<http://www.geodata.cn/>) for free public access. Now we temporarily upload a copy of our data as supporting information for review purposes.

<sup>1</sup>Supplemental Material. Table S1: GPS velocity data in a Eurasian-fixed Reference Frame (velocity in mm/yr); Table S2: GPS velocity data in a South China Block-fixed Reference Frame (velocity in mm/yr); Table S3: GPS stations in the South China Block used to define the Euler Vector for transformation of reference frame (velocity in mm/yr); Table S4: Interpolated velocities of the points on current fault trace and extension line of undeflected fault segment, and the averages of each pair of corresponding points (velocity in mm/yr); Table S5: Position and backward velocity of points on current fault trace (velocity in mm/yr); Table S6: Points inferred from the best estimate of duration time; Table S7: Points on smoothed original fault trace. Please visit <https://doi.org/10.1130/GSAB.S.14829453> to access the supplemental material, and contact editing@geosociety.org with any questions.

#### REFERENCES CITED

- Abdrakhmatov, K.Ye., Aldazhanov, S.A., Hager, B.H., Hamburger, M.W., Herring, T.A., Kalabaev, K.B., Makarov, V.I., Molnar, P., Panasyuk, S.V., Prilepin, M.T., Reilinger, R.E., Sadybakasov, I.S., Souter, B.J., Trapeznikov, Yu.A., Tsurkov, V.Ye., and Zubovich, A.V., 1996, Relatively recent construction of the Tien Shan inferred from GPS measurements of present-day crustal deformation rates: *Nature*, v. 384, p. 450–453, <https://doi.org/10.1038/384450a0>.
- Allen, C.R., Han, Y., Sieh, K.E., Zhang, B., and Zhu, C.N., 1984, Red River and associated faults, Yunnan Province, China: Quaternary geology, slip rate, and seismic hazard: *Geological Society of America Bulletin*, v. 95, p. 686–700, [https://doi.org/10.1130/0016-7606\(1984\)95<686:RRAAFY>2.0.CO;2](https://doi.org/10.1130/0016-7606(1984)95<686:RRAAFY>2.0.CO;2).
- Antolín, B., Schill, E., Grujic, D., Baule, S., Quidelleur, X., Appel, E., and Waldhör, M., 2012, E-W extension and block rotation of the southeastern Tibet: Unravelling late deformation stages in the eastern Himalayas (NW Bhutan) by means of pyrrhotite remanences: *Journal of Structural Geology*, v. 42, p. 19–33, <https://doi.org/10.1016/j.jsg.2012.07.003>.
- Armijo, R., Tappin, P., Mercier, L., and Han, T., 1986, Quaternary extension in southern Tibet: Field observations and tectonic implications: *Journal of Geophysical Research. Solid Earth*, v. 91, no. B14, p. 13803–13872, <https://doi.org/10.1029/JB091iB14p13803>.
- Avouac, J.P., Tappin, P., Bai, M., You, H., and Wang, G., 1993, Active thrusting and folding along the northern Tien Shan, and Late Cenozoic rotation of the Tarim relative to Dzungaria and Kazakhstan: *Journal of Geophysical Research. Solid Earth*, v. 98, p. 6755–6804, <https://doi.org/10.1029/92JB01963>.
- Bahadori, A., Holt, W.E., and Rasbury, E.T., 2018, Reconstruction modeling of crustal thickness and paleotopography of western North America since 36 Ma: *Geosphere*, v. 14, p. 1207–1231, <https://doi.org/10.1130/GES01604.1>.
- Bird, P., and Baumgardner, J., 1981, Steady propagation of delamination events: *Journal of Geophysical Research. Solid Earth*, v. 86, p. 4891–4903, <https://doi.org/10.1029/JB086iB06p04891>.
- Bird, P., and Piper, K., 1980, Plane stress finite element models of tectonic flow in southern California: Physics of the Earth and Planetary Interiors, v. 21, p. 158–175, [https://doi.org/10.1016/0031-9201\(80\)90067-9](https://doi.org/10.1016/0031-9201(80)90067-9).
- Blisniuk, P., Hacker, B., Glodny, J., Ratschbacher, L., Bi, S., Wu, Z., McWilliams, M., and Calvert, A., 2001, Normal faulting in central Tibet since at least 13.5 Myr ago: *Nature*, v. 412, no. 6847, p. 628–632, <https://doi.org/10.1038/35088045>.
- Bullen, M.E., Burbank, D.W., Garver, J.I., and Abdakhmatov, K.Ye., 2001, Late Cenozoic tectonic evolution of the northwestern Tien Shan: New age estimates for the initiation of mountain building: *Geological Society of America Bulletin*, v. 113, p. 1544–1559, [https://doi.org/10.1130/0016-7606\(2001\)113<1544:LCTEOT>2.0.CO;2](https://doi.org/10.1130/0016-7606(2001)113<1544:LCTEOT>2.0.CO;2).
- Bullen, M.E., Burbank, D.W., and Garver, J.I., 2003, Building the northern Tien Shan: Integrated thermal, structural, and topographic constraints: *The Journal of Geology*, v. 111, p. 149–165, <https://doi.org/10.1086/345840>.
- Burchfiel, B., and Chen, Z., 2012, Tectonics of the Southeastern Tibetan Plateau and its Adjacent Foreland: *Geological Society of America Memoir* 210, 231 p.
- Burchfiel, B., Zhiliang, C., Yuping, L., and Royden, L., 1995, Tectonics of the Longmen Shan and adjacent regions, central China: *International Geology Review*, v. 37, p. 661–735, <https://doi.org/10.1080/0026819509465424>.
- Chang, L.-J., Flesch, L.M., Wang, C.-Y., and Ding, Z.-F., 2015, Vertical coherence of deformation in lithosphere in the eastern Himalayan syntaxis using GPS, Quaternary fault slip rates, and shear wave splitting data: *Geophysical Research Letters*, v. 42, p. 5813–5819, <https://doi.org/10.1002/2015GL064568>.
- Charreau, J., Chen, Y., Gilder, S., Dominguez, S., Avouac, J.-P., Sen, S., Sun, D.-J., Li, Y.-A., and Wang, W.-M., 2005, Magnetostriatigraphy and rock magnetism of the Neogene Kuitun He Section (Northwest China): Implications for Late Cenozoic uplift of the

- Tianshan mountains: Earth and Planetary Science Letters, v. 230, p. 177–192, <https://doi.org/10.1016/j.epsl.2004.11.002>.
- Charreau, J., Avouac, J.-P., Chen, Y., Dominguez, S., and Gilder, S., 2008, Miocene to present kinematics of fault-bend folding across the Huerguosi anticline, northern Tianshan (China), derived from structural, seismic, and magnetostratigraphic data: *Geology*, v. 36, p. 871–874, <https://doi.org/10.1130/G25073A.1>.
- Charreau, J., Chen, Y., Gilder, S., Barrier, L., Dominguez, S., Augier, R., Sen, S., Avouac, J.-P., Gallaud, A., Gravelleau, F., and Wang, Q.-C., 2009, Neogene uplift of the Tian Shan Mountains observed in the magnetic record of the Jingou River section (northwest China): *Tectonics*, v. 28, no. 2, <https://doi.org/10.1029/2007TC002137>.
- Chen, H., Dobson, J., Heller, F., and Jie, H., 1995, Paleomagnetic evidence for clockwise rotation of the Simao region since the Cretaceous: A consequence of the India-Asia collision: *Earth and Planetary Science Letters*, v. 134, p. 203–217, [https://doi.org/10.1016/0012-821X\(95\)00118-V](https://doi.org/10.1016/0012-821X(95)00118-V).
- Chen, S., and Wilson, C.J.L., 1996, Emplacement of the Longmen Shan Thrust-Nappe Belt along the eastern margin of the Tibetan Plateau: *Journal of Structural Geology*, v. 18, p. 413–430, [https://doi.org/10.1016/0911-8141\(95\)00096-V](https://doi.org/10.1016/0911-8141(95)00096-V).
- Chevalier, M.L., Leloup, P.H., Replumaz, A., Pan, J., Métois, M., and Li, H., 2017, Temporally constant slip-rate along the Ganzi fault, NW Xianshuuhe fault system, eastern Tibet: *Geological Society of America Bulletin*, v. 130, p. 396–410, <https://doi.org/10.1130/B31691.1>.
- Clark, M.K., and Royden, L.H., 2000, Topographic ooze: Building the eastern margin of Tibet by lower crustal flow: *Geology*, v. 28, p. 703–706, [https://doi.org/10.1130/0091-7613\(2000\)28<703:TOBTEM>2.0.CO;2](https://doi.org/10.1130/0091-7613(2000)28<703:TOBTEM>2.0.CO;2).
- Clark, M.K., House, M.A., Royden, L.H., Whipple, K.X., Burchfiel, B.C., Zhang, X., and Tang, W., 2005, Late Cenozoic uplift of southeastern Tibet: *Geology*, v. 33, p. 525–528, <https://doi.org/10.1130/G21265.1>.
- Cobbold, P.R., and Davy, P., 1988, Indentation tectonics in nature and experiment. 2. Central Asia: *Bulletin of the Geological Institution of the University of Uppsala*, v. 14, p. 143–162.
- Copley, A., and McKenzie, D., 2007, Models of crustal flow in the India-Asia collision zone: *Geophysical Journal International*, v. 169, p. 683–698, <https://doi.org/10.1111/j.1365-246X.2007.03343.x>.
- Davis, P., England, P., and Houseman, G., 1997, Comparison of shear wave splitting and finite strain from the India-Asia collision zone: *Journal of Geophysical Research: Solid Earth*, v. 102, p. 27511–27522, <https://doi.org/10.1029/97JB02378>.
- Davy, P., and Cobbold, P.R., 1988, Indentation tectonics in nature and experiment. 1. Experiments scaled for gravity: *Bulletin of the Geological Institution of the University of Uppsala*, v. 14, p. 129–141.
- DeMets, C., and Merkouriev, S., 2016, High-resolution reconstructions of Pacific–North America plate motion: 20 Ma to present: *Geophysical Journal International*, v. 207, p. 741–773, <https://doi.org/10.1093/gji/ggw305>.
- DeMets, C., and Merkouriev, S., 2019, High-resolution reconstructions of South America plate motion relative to Africa, Antarctica and North America: 34 Ma to present: *Geophysical Journal International*, v. 217, p. 1821–1853, <https://doi.org/10.1093/gji/ggz087>.
- DeMets, C., Gordon, R.G., and Royer, J.-Y., 2005, Motion between the Indian, Capricorn and Somalian plates since 20 Ma: Implications for the timing and magnitude of distributed lithospheric deformation in the equatorial Indian ocean: *Geophysical Journal International*, v. 161, p. 445–468, <https://doi.org/10.1111/j.1365-246X.2005.02598.x>.
- DeMets, C., Iaffaldano, G., and Merkouriev, S., 2015a, High-resolution Neogene and Quaternary estimates of Nubia-Eurasia-North America Plate motion: *Geophysical Journal International*, v. 203, p. 416–427, <https://doi.org/10.1093/gji/ggv277>.
- DeMets, C., Merkouriev, S., and Sauter, D., 2015b, High-resolution estimates of Southwest Indian Ridge plate motions, 20 Ma to present: *Geophysical Journal International*, v. 203, p. 1495–1527, <https://doi.org/10.1093/gji/gjv366>.
- DeMets, C., Merkouriev, S., and Jade, S., 2020, High-resolution reconstructions and GPS estimates of India-Eurasia and India-Somalia plate motions: 20 Ma to the present: *Geophysical Journal International*, v. 220, p. 1149–1171, <https://doi.org/10.1093/gji/ggz508>.
- Devachandra, M., Kundu, B., Catherine, J., and Arun Kumar, A., 2014, Global positioning system (GPS) measurements of crustal deformation across the frontal eastern Himalayan syntaxis and seismic-hazard assessment: *Bulletin of the Seismological Society of America*, v. 104, no. 3, p. 1518–1524, <https://doi.org/10.1785/0120130290>.
- Dewane, T., Stockli, D., Hager, C., Taylor, M., Ding, L., Lee, J., and Wallis, S., 2006, Timing of Cenozoic E-W extension in the Tangra Yun Co-Kung rift, south-central Tibet: American Geophysical Union, Fall Meeting, Abstract T34C-04.
- Duong, N., Sagiya, T., Kimata, F., To, T., Hai, V., Cong, D., Binh, N., and Xuyen, N., 2013, Contemporary horizontal crustal movement estimation for northwestern Vietnam inferred from repeated GPS measurements: *Earth, Planets, and Space*, v. 65, no. 12, p. 1399–1410, <https://doi.org/10.5047/eps.2013.09.010>.
- Dupont-Nivet, G., Horton, B.K., Butler, R.F., Wang, J., Zhou, J., and Waanders, G.L., 2004, Paleogene clockwise tectonic rotation of the Xining-Lanzhou region, northeastern Tibetan Plateau: *Journal of Geophysical Research: Solid Earth*, v. 109, no. 4, <https://doi.org/10.1029/2003JB002620>.
- Dupont-Nivet, G., Dai, S., Fang, X., Krijgsman, W., Erens, V., Reitsma, M., and Langereis, C., 2008, Timing and distribution of tectonic rotations in the northeastern Tibetan Plateau, in Burchfiel, B.C., and Wang, E., eds., *Investigations into the Tectonics of the Tibetan Plateau: Geological Society of America Special Paper 444*, 73–87, [https://doi.org/10.1130/2008.2444\(05\)](https://doi.org/10.1130/2008.2444(05)).
- Duvall, A.R., and Clark, M.K., 2010, Dissipation of fast strike-slip faulting within and beyond northeastern Tibet: *Geology*, v. 38, p. 223–226, <https://doi.org/10.1130/G30711.1>.
- Edwards, M.A., and Harrison, T.M., 1997, When did the roof collapse? Late Miocene north-south extension in the high Himalaya revealed by Th-Pb monazite dating of the Khula Kangri granite: *Geology*, v. 25, no. 6, p. 543–546, [https://doi.org/10.1130/0091-7613\(1997\)025<0543:WDTRCL>2.3.CO;2](https://doi.org/10.1130/0091-7613(1997)025<0543:WDTRCL>2.3.CO;2).
- Elliott, J.R., Walters, R.J., England, P.C., Jackson, J.A., Li, Z., and Parsons, B., 2010, Extension on the Tibetan plateau: Recent normal faulting measured by InSAR and body wave seismology: *Geophysical Journal International*, v. 183, no. 2, p. 503–535, <https://doi.org/10.1111/j.1365-246X.2010.04754.x>.
- England, P., and McKenzie, D., 1982, A thin viscous sheet model for continental deformation: *Geophysical Journal of the Royal Astronomical Society*, v. 70, p. 295–321, <https://doi.org/10.1111/j.1365-246X.1982.tb04969.x>.
- England, P., and McKenzie, D., 1983, Correction to: A thin viscous sheet model for continental deformation: *Geophysical Journal of the Royal Astronomical Society*, v. 73, p. 523–532, <https://doi.org/10.1111/j.1365-246X.1983.tb0328.x>.
- England, P., and Houseman, G., 1986, Finite strain calculations of continental deformation 2. Comparison with the India-Asia collision zone: *Journal of Geophysical Research: Solid Earth*, v. 91, p. 3664–3676, <https://doi.org/10.1029/JB091iB03p03664>.
- England, P., and Houseman, G., 1989, Extension during continental convergence, with application to the Tibetan Plateau: *Journal of Geophysical Research: Solid Earth*, v. 94, p. 17561–17579, <https://doi.org/10.1029/JB094iB12p17561>.
- England, P., and Molnar, P., 1990, Right-lateral shear and rotation as the explanation for strike-slip faulting in eastern Tibet: *Nature*, v. 344, p. 140–142, <https://doi.org/10.1038/344140a0>.
- England, P., and Molnar, P., 1997, Active deformation of Asia: From kinematics to dynamics: *Science*, v. 278, p. 647–650, <https://doi.org/10.1126/science.278.5338.647>.
- England, P., Houseman, G., and Noqué, J.-M., 2016, Constraints from GPS measurements on the dynamics of deformation in Anatolia and the Aegean: *Journal of Geophysical Research: Solid Earth*, v. 121, p. 8888–8916, <https://doi.org/10.1002/2016JB013382>.
- Fang, X., Garzione, C., Van der Voo, R., Li, J., and Fan, M., 2003, Flexural subsidence by 29 Ma on the NE edge of Tibet from the magnetostratigraphy of Linxia Basin, China: *Earth and Planetary Science Letters*, v. 210, p. 545–560, [https://doi.org/10.1016/S0012-821X\(03\)00142-0](https://doi.org/10.1016/S0012-821X(03)00142-0).
- Flesch, L.M., Holt, W.E., Haines, A.J., and Shen-Tu, B., 2000, Dynamics of the Pacific-North American plate boundary in the western United States: *Science*, v. 287, p. 834–836, <https://doi.org/10.1126/science.287.5454.834>.
- Flesch, L.M., Haines, A.J., and Holt, W.E., 2001, Dynamics of the India-Eurasia collision zone: *Journal of Geophysical Research: Solid Earth*, v. 106, p. 16435–16460, <https://doi.org/10.1029/2001JB000208>.
- Flesch, L.M., Holt, W.E., Silver, P.G., Stephenson, M., Wang, C.-Y., and Chan, W.W., 2005, Constraining the extent of crust upper mantle coupling in central Asia using GPS, geologic, and shear-wave splitting data: *Earth and Planetary Science Letters*, v. 238, p. 248–268, <https://doi.org/10.1016/j.epsl.2005.06.023>.
- Funahara, S., Nishiwaki, N., Miki, M., Murata, F., Otofuji, Y.-I., and Wang, Y.Z., 1992, Paleomagnetic study of Cretaceous rocks from the Yangtze block, central Yunnan, China: Implications for the India-Asia collision: *Earth and Planetary Science Letters*, v. 113, p. 77–91.
- Funahara, S., Nishiwaki, N., Murata, F., Otofuji, Y.-I., and Wang, Y.Z., 1993, Clockwise rotation of the Red River fault inferred from paleomagnetic study of the Cretaceous rocks in the Shan-Thai-Malay block of western Yunnan, China: *Earth and Planetary Science Letters*, v. 117, p. 29–42, [https://doi.org/10.1016/0012-821X\(93\)90115-P](https://doi.org/10.1016/0012-821X(93)90115-P).
- Fyhn, M.B.W., and Phach, P.V., 2015, Late Neogene structural inversion around the northern Gulf of Tonkin, Vietnam: Effects from right-lateral displacement across the Red River fault zone: *Tectonics*, v. 34, p. 290–312, <https://doi.org/10.1002/2014TC003674>.
- Gan, W., Zhang, P., Shen, Z., Niu, Z., Wang, M., Wan, Y., Zhou, D., and Cheng, J., 2007, Present-day crustal motion within the Tibetan Plateau inferred from GPS measurements: *Journal of Geophysical Research: Solid Earth*, v. 112, p. 582–596, <https://doi.org/10.1029/2005JB004120>.
- Garzione, C., DeCelles, P., Hodkinson, D., Ojha, T., and Upreti, B., 2003, East-west extension and Miocene environmental change in the southern Tibetan plateau: Thakkola graben, central Nepal: *Geological Society of America Bulletin*, v. 115, no. 1, p. 3–20, [https://doi.org/10.1130/0016-7606\(2003\)115<0003:EWEAME>2.0.CO;2](https://doi.org/10.1130/0016-7606(2003)115<0003:EWEAME>2.0.CO;2).
- Garzione, C.N., Molnar, P., Libarkin, J.C., and MacFadden, B.J., 2006, Rapid Late Miocene rise of the Bolivian Altiplano: Evidence for removal of mantle lithosphere: *Earth and Planetary Science Letters*, v. 241, p. 543–556, <https://doi.org/10.1016/j.epsl.2005.11.026>.
- Garzione, C.N., Hoke, G.D., Libarkin, J.C., Withers, S., MacFadden, B., Eiler, J., Ghosh, P., and Mulch, A., 2008, Rise of the Andes: *Science*, v. 320, p. 1304–1307, <https://doi.org/10.1126/science.1148615>.
- Ge, W., Molnar, P., Shen, Z., and Li, Q., 2015, Present-day crustal thinning in the southern and northern Tibetan Plateau revealed by GPS measurements: *Geophysical Research Letters*, v. 42, p. 5227–5235, <https://doi.org/10.1002/2015GL064347>.
- Godard, V., Pik, R., Lavé, J., Cattin, R., Tibari, B., de Sigoyer, J., Pubellier, M., and Zhu, J., 2009, Late Cenozoic evolution of the central Longmen Shan, eastern Tibet: Insight from (U-Th)/He thermochronometry: *Tectonics*, v. 28, no. 5, <https://doi.org/10.1029/2008TC002407>.
- Godard, V., Lavé, J., Carcaillet, J., Cattin, R., Bourlès, D., and Zhu, J., 2010, Spatial distribution of denudation in eastern Tibet and regressive erosion of plateau margins: *Tectonophysics*, v. 491, p. 253–274, <https://doi.org/10.1016/j.tecto.2009.10.026>.
- Gubbels, T., Isacks, B., and Farrar, E., 1993, High level surfaces, plateau uplift, and foreland basin development, Bolivian central Andes: *Geology*, v. 21, p. 695–698, [https://doi.org/10.1130/0091-7603\(1993\)021<695:HLSPAU>2.3.CO;2](https://doi.org/10.1130/0091-7603(1993)021<695:HLSPAU>2.3.CO;2).

- doi.org/10.1130/0091-7613(1993)021<0695:HLSPUA>2.3.CO;2.
- Gupta, T., Riguzzi, F., Dasgupta, S., Mukhopadhyay, B., Roy, S., and Sharma, S., 2015, Kinematics and strain rates of the Eastern Himalayan Syntaxis from new GPS campaigns in Northeast India: Tectonophysics, v. 655, p. 15–26, https://doi.org/10.1016/j.tecto.2015.04.017.
- Harrison, T., Leloup, P., Ryerson, F., Tapponnier, P., Lacassin, R., and Chen, W., 1996, Diachronous initiation of transtension along the Ailao Shan-Red River shear zone, Yunnan and Vietnam: World and Regional Geology, p. 208–226.
- Harrison, T.M., Copeland, P., Kidd, W.S.F., and Yin, A., 1992, Raising Tibet: Science, v. 255, p. 1663–1670, https://doi.org/10.1126/science.255.5052.1663.
- Harrison, T.M., Copeland, P., Kidd, W.S.F., and Lovera, O.M., 1995, Activation of the Nyainqntanglha shear zone: Implications for uplift of the southern Tibetan Plateau: Tectonics, v. 14, no. 3, p. 658–676, https://doi.org/10.1029/95TC00608.
- Holt, W.E., 2000, Correlated crust and mantle strain fields in Tibet: Geology, v. 28, p. 67–70, https://doi.org/10.1130/0091-7613(2000)28<67:CCAMSF>2.0.CO;2.
- Holt, W.E., and Haines, A.J., 1993, Velocity fields in deforming Asia from the inversion of earthquake-released strains: Tectonics, v. 12, p. 1–20, https://doi.org/10.1029/92TC00658.
- Holt, W.E., Ni, J.F., Wallace, T.C., and Haines, A.J., 1991, The active tectonics of the Eastern Himalayan Syntaxis and surrounding regions: Journal of Geophysical Research: Solid Earth, v. 96, p. 14595–14632, https://doi.org/10.1029/91JB01021.
- Hough, B.G., Garzione, C.N., Wang, Z.C., Lease, R.O., Burbank, D.W., and Yuan, D.Y., 2011, Stable isotope evidence for topographic growth and basin segmentation: Implications for the evolution of the NE Tibetan plateau: Geological Society of America Bulletin, v. 123, p. 168–185, https://doi.org/10.1130/B30090.1.
- Houseman, G., and England, P., 1986, Finite strain calculations of continental deformation: I. Method and general results for convergent zones: Journal of Geophysical Research: Solid Earth, v. 91, p. 3651–3663, https://doi.org/10.1029/9JB091iB03p03651.
- Houseman, G.A., McKenzie, D.P., and Molnar, P., 1981, Convective instability of a thickened boundary layer and its relevance for the thermal evolution of continental convergent belts: Journal of Geophysical Research: Solid Earth, v. 86, p. 6115–6132, https://doi.org/10.1029/JB086iB07p06115.
- Huang, K.-N., and Opdyke, N.D., 1992, Paleomagnetism of Cretaceous to Lower Tertiary rocks from Southwestern Sichuan: A revisit: Earth and Planetary Science Letters, v. 112, p. 29–40, https://doi.org/10.1016/0012-821X(92)90004-F.
- Huang, K.-N., and Opdyke, N.D., 1993, Paleomagnetic results from Cretaceous and Jurassic rocks of South and Southwest Yunnan: Evidence for large clockwise rotations in the Indochina and Shan-Thai-Malay terranes: Earth and Planetary Science Letters, v. 117, p. 507–524, https://doi.org/10.1016/0012-821X(93)90100-N.
- Huang, K.-N., Opdyke, N.D., Li, J.-G., and Peng, X.-J., 1992, Paleomagnetism of Cretaceous rocks from eastern Qiangtang terrane of Tibet: Journal of Geophysical Research: Solid Earth, v. 97, p. 1789–1799, https://doi.org/10.1029/91JB02747.
- Huang, B.-C., Piper, J.D.A., Peng, S.-T., Liu, T., Li, Z., Wang, Q.-C., and Zhu, R.-X., 2006, Magnetostratigraphic study of the Kuche Depression, Tarim Basin, and Cenozoic uplift of the Tian Shan Range, western China: Earth and Planetary Science Letters, v. 251, p. 346–364, https://doi.org/10.1016/j.epsl.2006.09.020.
- Huang, B.-C., Piper, J.D.A., Qiao, Q.-Q., Wang, H.-I., and Zhang, C.-X., 2010, Magnetostratigraphic and rock magnetic study of the Neogene upper Yaha section, Kuche Depression (Tarim Basin): Implications to formation of the Xiyu conglomerate formation, NW China: Journal of Geophysical Research: Solid Earth, v. 115, no. B1, https://doi.org/10.1029/2008JB006175.
- Hubbard, J., and Shaw, J.H., 2009, Uplift of the Longmen Shan and Tibetan plateau, and the 2008 Wenchuan (M = 7.9) earthquake: Nature, v. 458, p. 194–197, https://doi.org/10.1038/nature07837.
- Iaffaldano, G., 2014, A geodynamical view on the steadiness of geodetically derived rigid plate motions over geological time: Geochemistry, Geophysics, Geosystems, v. 15, p. 238–254, https://doi.org/10.1002/2013GC005088.
- Iaffaldano, G., Bunge, H.-P., and Dixon, T.H., 2006, Feedback between mountain belt growth and plate convergence: Geology, v. 34, p. 893–896, https://doi.org/10.1130/G22661.1.
- Iaffaldano, G., Hawkins, R., and Cambridge, M., 2014, Bayesian noise reduction in Arabia/Somalia and Nubia/Arabia finite rotations since ~20 Ma: Implications for Nubia/Somalia relative motion: Geochemistry, Geophysics, Geosystems, v. 15, p. 845–854, https://doi.org/10.1002/2013GC005089.
- Jessup, M.J., and Cottle, J.M., 2010, Progression from south-directed extrusion to orogen-parallel extension in the Southern Margin of the Tibetan Plateau, Mount Everest region, Tibet: The Journal of Geology, v. 118, no. 5, p. 467–486, https://doi.org/10.1086/655011.
- Ji, J.-L., Luo, P., White, P., Jiang, H.-C., Gao, L., and Ding, Z.-L., 2008, Episodic uplift of the Tianshan Mountains since the late Oligocene constrained by magnetostratigraphy of the Junggar River section, in the southern margin of the Junggar Basin, China: Journal of Geophysical Research: Solid Earth, v. 113, no. B5, https://doi.org/10.1029/2007JB005064.
- Kapp, P., and DeCelles, P.G., 2019, Mesozoic-Cenozoic geological evolution the Himalayan-Tibetan orogen and working tectonic hypotheses: American Journal of Science, v. 319, no. 3, p. 159–254, https://doi.org/10.2475/03.2019.01.
- Kennan, L., Lamb, S., and Hoke, L., 1997, High altitude paleosurfaces in the Bolivian Andes: Evidence for late Cenozoic surface uplift, in Widdowson, M., ed., Paleosurfaces: Recognition, Reconstruction and Paleoenvironmental Interpretation: Geological Society of London Special Publication 120, p. 307–324.
- Kali, E., Leloup, P.H., Arnaud, N., Mahéo, G., Liu, D., Boutonnet, E., Van der Woerd, J., Liu, X., Liu-Zeng, J., and Li, H., 2010, Exhumation history of the deepest central Himalayan rocks, Ama Drime range: Key pressure-temperature-deformation-time constraints on orogenic models: Tectonics, v. 29, no. 2, https://doi.org/10.1029/2009TC002551.
- Kornfeld, D., Eckert, S., Appel, E., Ratschbacher, L., Pfänder, J., Liu, D.-I., and Ding, L., 2014, Clockwise rotation of the Baoshan Block due to southeastward tectonic escape of Tibetan crust since the Oligocene: Geophysical Journal International, v. 197, p. 149–163, https://doi.org/10.1093/gji/ggu009.
- Krijgsman, W., Hilgen, F.J., Raffi, I., Sierra, F.J., and Wilson, D.S., 1999, Chronology, causes and progression of the Messinian salinity crisis: Nature, v. 400, p. 652–655, https://doi.org/10.1038/23231.
- Lamb, S.H., 1987, A model for tectonic rotations about a vertical axis: Earth and Planetary Science Letters, v. 84, p. 75–86, https://doi.org/10.1016/0012-821X(87)90178-6.
- Lease, R.O., Burbank, D.W., Clark, M.K., Farley, K.A., Zheng, D., and Zhang, H., 2011, Middle Miocene reorganization of deformation along the northeastern Tibetan Plateau: Geology, v. 39, no. 4, p. 359–362, https://doi.org/10.1130/G31356.1.
- Lee, J., Hager, C., Wallis, S.R., Stockli, D.F., Whitehouse, M.J., Aoya, M., and Wang, Y., 2011, Middle to late Miocene extremely rapid exhumation and thermal reequilibration in the Kung Co rift, southern Tibet: Tectonics, v. 30, no. 2, https://doi.org/10.1029/2010TC002745.
- Leloup, P., Arnaud, N., Lacassan, R., Kienast, J., Harrison, T., Trong, T., Replumaz, A., and Tapponnier, P., 2001, New constraints on the structure, thermochronology, and timing of the Ailao Shan-Red River shear zone, SE Asia: Journal of Geophysical Research: Solid Earth, v. 106, p. 6683–6732, https://doi.org/10.1029/2000JB900322.
- Li, M., Xing, C., Cai, C., Guo, W., Wu, S., Yuan, Z., Meng, Y., Tu, D., Zhang, R., and Zhou, R., 1995, Research on activity of Yushu fault: Dizhen Dizhi, v. 17, p. 218–224.
- Li, Q., You, X., Yang, S., Du, R., Qiao, X., Zou, R., and Wang, Q., 2012, A precise velocity field of tectonic deformation in China as inferred from intensive GPS observations: Science China. Earth Sciences, v. 55, no. 5, p. 695–698, https://doi.org/10.1007/s11430-012-4412-5.
- Li, S.-H., Deng, C.-L., Dong, W., Sun, L., Liu, S.-Z., Qin, H.-F., Yin, J.-Y., Ji, X.-P., and Zhu, R.-X., 2015, Magnetostratigraphy of the Xiaolongtan Formation bearing *Lufengpithecus keiyuanensis* in Yunnan, southwestern China: Constraint on the initiation time of the southern segment of the Xianshuhe-Xiaojiang fault: Tectonophysics, v. 655, p. 213–226, https://doi.org/10.1016/j.tecto.2015.06.002.
- Li, S.-H., van Hinsbergen, D.J.J., Deng, C.-L., Advokaat, E.L., and Zhu, R.-X., 2018, Paleomagnetic constraints from the Baoshan area on the deformation of the Qiangtang-Sibumasu terrane around the eastern Himalayan syntaxis: Journal of Geophysical Research: Solid Earth, v. 123, p. 977–997, https://doi.org/10.1002/2017JB015112.
- Li, Y., Allen, P.A., Densmore, A.L., and Qiang, X., 2003, Evolution of the Longmen Shan Foreland Basin (western Sichuan, China) during the Late Triassic Indosinian Orogeny: Basin Research, v. 15, p. 117–138, https://doi.org/10.1046/j.1365-2117.2003.00197.x.
- Li, Z., Wang, Y., Gan, W., Fang, L., Zhou, R., Seagren, E.G., Zhang, H., Liang, S., Zhuang, W., and Yang, F., 2020, Diffuse deformation in the SE Tibetan Plateau: New insights from geodetic observations: Journal of Geophysical Research: Solid Earth, v. 125, no. 10, https://doi.org/10.1029/2020JB019383.
- Liang, S.M., Gan, W.J., Shen, C.Z., Xiao, G.R., Liu, J., Chen, W., Ding, X., and Zhou, D., 2013, Three-dimensional velocity field of present-day crustal motion of the Tibetan plateau derived from GPS measurements: Journal of Geophysical Research: Solid Earth, v. 118, no. 10, p. 5722–5732, https://doi.org/10.1002/2013JB010503.
- Liu, J., Yang, Z.-Y., Tong, Y.-B., Yuan, W., and Wang, B., 2010, Tectonic implications of early-middle Triassic palaeomagnetic results from Hexi Corridor, North China: Geophysical Journal International, v. 182, p. 1216–1228, https://doi.org/10.1111/j.1365-246X.2010.04699.x.
- Liu-Zeng, J., Tapponnier, P., Gaudemer, Y., and Ding, L., 2008, Quantifying landscape differences across the Tibetan plateau: Implications for topographic relief evolution: Journal of Geophysical Research: Earth Surface, v. 113, no. F4, https://doi.org/10.1029/2007JF000897.
- Macaulay, E.A., Sobel, E.R., Mikolaichuk, A., Landgraf, A., Kohn, B., and Stuart, F., 2013, Thermochronologic insight into late Cenozoic deformation in the basement-cored Terskey Range, Kyrgyz Tien Shan: Tectonics, v. 32, p. 487–500, https://doi.org/10.1002/tect.20040.
- McKenzie, D., and Priestley, K., 2008, The influence of lithospheric thickness variations on continental evolution: Lithos, v. 102, p. 1–11, https://doi.org/10.1016/j.lithos.2007.05.005.
- Merkouriev, S., and DeMets, C., 2006, Constraints on Indian plate motion since 20 Ma from dense Russian magnetic data: Implications for Indian plate dynamics: Geochemistry, Geophysics, Geosystems, v. 7, no. 2, https://doi.org/10.1029/2005GC001079.
- Merkouriev, S., and DeMets, C., 2008, A high-resolution model for Eurasia-North America plate kinematics since 20 Ma: Geophysical Journal International, v. 173, p. 1064–1083, https://doi.org/10.1111/j.1365-246X.2008.03761.x.
- Merkouriev, S., and DeMets, C., 2014, High-resolution estimates of Nubia–North America plate motion: 20 Ma to present: Geophysical Journal International, v. 196, p. 1281–1298, https://doi.org/10.1093/gji/ggt463.
- McCallister, A., Taylor, M., Murphy, M., Styron, R., and Stockli, D., 2014, Thermochronologic constraints on the late Cenozoic exhumation history of the Gurla Mandhata metamorphic core complex, Southwestern Tibet: Tectonics, v. 33, no. 2, p. 27–52, https://doi.org/10.1002/2013TC003302.
- McKenzie, D., and Jackson, J., 1983, The relationship between strain rates, crustal thickening, paleomagnetism, finite strain and fault movements within a deforming zone: Earth and Planetary Science Letters, v. 65, p. 182–202, https://doi.org/10.1016/0012-821X(83)90198-X.
- Molnar, P., and Chen, W.P., 1983, Focal depths and fault plane solutions of earthquakes under the Tibetan plateau:

- Journal of Geophysical Research. Solid Earth, v. 88, p. 1180–1196, <https://doi.org/10.1029/JB088iB02p01180>.
- Molnar, P., and Lyon-Caen, H., 1989, Fault plane solutions of earthquakes and active tectonics of the Tibetan Plateau and its margins: *Geophysical Journal International*, v. 99, no. 1, p. 123–153, <https://doi.org/10.1111/j.1365-246X.1989.tb02020.x>.
- Molnar, P., and Stock, J.M., 2009, Slowing of India's convergence with Eurasia since 20 Ma and its implications for Tibetan mantle dynamics: *Tectonics*, v. 28, no. 3, <https://doi.org/10.1029/2008TC002271>.
- Molnar, P., and Tapponnier, P., 1978, Active tectonics of Tibet: *Journal of Geophysical Research. Solid Earth*, v. 83, p. 5361–5375, <https://doi.org/10.1029/JB083iB11p05361>.
- Molnar, P., England, P., and Martinod, J., 1993, Mantle dynamics, uplift of the Tibetan Plateau, and the Indian monsoon: *Reviews of Geophysics*, v. 31, p. 357–396, <https://doi.org/10.1029/93RG02030>.
- Murphy, M.A., Yin, A., Kapp, P., Harrison, T.M., Manning, C.E., Ryerson, F.J., Ding, L., and Guo, J.H., 2002, Structural evolution of the Gurla Mandhata detachment system, southwest Tibet: implications for the eastward extent of the Karakoram fault system: *Geological Society of America Bulletin*, v. 114, no. 4, p. 428–447, [https://doi.org/10.1130/0016-7606\(2002\)114<0428:SEOTGM>2.0.CO;2](https://doi.org/10.1130/0016-7606(2002)114<0428:SEOTGM>2.0.CO;2).
- Ni, J., and York, J.E., 1978, Late Cenozoic tectonics of the Tibetan plateau: *Journal of Geophysical Research. Solid Earth*, v. 83, no. B11, p. 5377–5384, <https://doi.org/10.1029/JB083iB11p05377>.
- Otofuji, Y., Inoue, Y., Funahara, S., Murata, F., and Zheng, X., 1990, Palaeomagnetic study of eastern Tibet-deformation of the Three Rivers region: *Geophysical Journal International*, v. 103, p. 85–94, <https://doi.org/10.1111/j.1365-246X.1990.tb01754.x>.
- Otofuji, Y., Liu, Y.-Y., Yokoyama, M., Tamai, M., and Yin, J.-Y., 1998, Tectonic deformation of the southwestern part of the Yangtze craton inferred from paleomagnetism: *Earth and Planetary Science Letters*, v. 156, p. 47–60, [https://doi.org/10.1016/S0012-821X\(98\)00009-0](https://doi.org/10.1016/S0012-821X(98)00009-0).
- Otofuji, Y.-I., Yokoyama, M., Kitada, K., and Zaman, H., 2010, Paleomagnetic versus GPS determined tectonic rotation around eastern Himalayan syntaxis in East Asia: *Journal of Asian Earth Sciences*, v. 37, p. 438–451, <https://doi.org/10.1016/j.jseaes.2009.11.003>.
- Quimet, W., Whipple, K., Royden, L., Reiners, P., Hodges, K., and Pringle, M., 2010, Regional incision of the eastern margin of the Tibetan Plateau: *Lithosphere*, v. 2, no. 1, p. 50–63, <https://doi.org/10.1130/L57.1>.
- Pan, Y., and Kidd, W.S.F., 1992, Nyainqntanglha shear zone: A late Miocene extensional detachment in the southern Tibetan Plateau: *Geology*, v. 20, p. 775–778, [https://doi.org/10.1130/0091-7613\(1992\)020<0775:NSZALM>2.3.CO;2](https://doi.org/10.1130/0091-7613(1992)020<0775:NSZALM>2.3.CO;2).
- Qiao, Q.-Q., Huang, B.-C., Piper, J.D.A., Deng, T., and Liu, C.-Y., 2016, Neogene magnetostratigraphy and rock magnetic study of the Kash Depression, NW China: Implications to neotectonics in the SW Tianshan Mountains: *Journal of Geophysical Research. Solid Earth*, v. 121, p. 1280–1296, <https://doi.org/10.1002/2015JB012687>.
- Reitman, N. G., and Molnar, P., 2021, Strain and velocity across the Great Basin derived from 15-ka fault slip rates: Implications for continuous deformation and seismic hazard in the Walker Lane, California-Nevada, USA: *Tectonics*, v. 40, no. 3, <https://doi.org/10.1029/2020TC006389>.
- Replumaz, A., Lacassin, R., Tapponnier, P., and Leloup, P., 2001, Large river offsets and Plio-Quaternary dextral slip rate on the Red River fault (Yunnan, China): *Journal of Geophysical Research. Solid Earth*, v. 106, p. 819–836, <https://doi.org/10.1029/2000JB900135>.
- Roger, F., Calassou, S., Lancelot, J., Malavielle, M., Xu, Z., Hao, Z., and Hou, L., 1995, Miocene emplacement and deformation of the Konga Shan granite (Xianshuhe fault, West Sichuan, China): Geodynamic implications: *Earth and Planetary Science Letters*, v. 130, p. 201–216, [https://doi.org/10.1016/0012-821X\(94\)00252-T](https://doi.org/10.1016/0012-821X(94)00252-T).
- Royden, L.H., Burchfiel, B.C., King, R.W., Chen, Z., Shen, F., and Liu, Y., 1997, Surface deformation and lower crustal flow in eastern Tibet: *Science*, v. 276, p. 788–790, <https://doi.org/10.1126/science.276.5313.788>.
- Sanchez, V.I., Murphy, M.A., Robinson, A.C., Lapen, T.J., and Heizler, M.T., 2013, Tectonic evolution of the India-Asia suture zone since middle Eocene time, Lopukangri area, south-central Tibet: *Journal of Asian Earth Sciences*, v. 62, p. 205–220, <https://doi.org/10.1016/j.jseaes.2012.09.004>.
- Sato, K., Liu, Y.-Y., Zhu, Z.-C., Yang, Z.-Y., and Otofuji, Y.-I., 1999, Paleomagnetic study of middle Cretaceous rocks from Yunlong, western Yunnan, China: Evidence of southward displacement of Indochina: *Earth and Planetary Science Letters*, v. 165, p. 1–15, [https://doi.org/10.1016/S0012-821X\(98\)00257-X](https://doi.org/10.1016/S0012-821X(98)00257-X).
- Sato, K., Liu, Y.-Y., Zhu, Z.-C., Yang, Z.-Y., and Otofuji, Y.-I., 2001, Tertiary paleomagnetic data from northwestern Yunnan, China: Further evidence for large clockwise rotation of the Indochina block and its tectonic implications: *Earth and Planetary Science Letters*, v. 185, no. 1–2, p. 185–198, [https://doi.org/10.1016/S0012-821X\(00\)0377-0](https://doi.org/10.1016/S0012-821X(00)0377-0).
- Saylor, J., DeCelles, P., Gehrels, G., Murphy, M., Zhang, R., and Kapp, P., 2010, Basin formation in the High Himalaya by arc-parallel extension and tectonic damming: Zhada Basin, southwestern Tibet: *Tectonics*, v. 29, no. 1, <https://doi.org/10.1029/2008TC002390>.
- Schildgen, T.F., Hodges, K.V., Whipple, K.X., Reiners, P.W., and Pringle, M.S., 2007, Uplift of the western margin of the Andean plateau revealed from canyon incision history, southern Peru: *Geology*, v. 35, p. 523–526, <https://doi.org/10.1130/G23532A.1>.
- Schoenbohm, L., Burchfiel, B., Chen, L., and Yin, J., 2006, Miocene to present activity along the Red River fault, China, in the context of continental extrusion, upper-crustal rotation, and lower-crustal flow: *Geological Society of America Bulletin*, v. 118, no. 5–6, p. 672–688, <https://doi.org/10.1130/B25816.1>.
- Searle, M.P., Yeh, M.-W., Lin, T.-H., and Chung, S.-L., 2010, Structural constraints on the timing of left-lateral shear along the Red River shear zone in the Ailao Shan and Diancang Shan Ranges, Yunnan, SW China: *Geosphere*, v. 6, p. 316–338, <https://doi.org/10.1130/GES00580.1>.
- Searle, M.P., Roberts, N.M.W., Chung, S.-L., Lee, Y.-H., Cook, K.L., Elliott, J.R., Weller, O.M., St-Onge, M.R., Xu, X.-W., Tan, X.-B., and Li, K., 2016, Age and anatomy of the Gongga Shan batholith, eastern Tibetan Plateau, and its relationship to the active Xianshui-he fault: *Geosphere*, v. 12, p. 948–970, <https://doi.org/10.1130/GES01244.1>.
- Shen, Z.-K., Lü, J., Wang, M., and Bürgmann, R., 2005, Contemporary crustal deformation around the southeast borderland of the Tibetan Plateau: *Journal of Geophysical Research. Solid Earth*, v. 110, no. B11, <https://doi.org/10.1029/2004JB003421>.
- Sonder, L.J., and England, P., 1986, Vertical averages of rheology of the continental lithosphere: Relation to thin sheet parameters: *Earth and Planetary Science Letters*, v. 77, p. 81–90, [https://doi.org/10.1016/0012-821X\(86\)90134-2](https://doi.org/10.1016/0012-821X(86)90134-2).
- Styron, R.H., Taylor, M.H., Sundell, K.E., Stockli, D.F., Oallmann, J.A.G., Möller, A., McCallister, A.T., Liu, D.-L., and Ding, L., 2013, Miocene initiation and acceleration of extension in the South Lunggar rift, western Tibet: Evolution of an active detachment system from structural mapping and (U-Th)/He thermochronology: *Tectonics*, v. 32, p. 880–907, <https://doi.org/10.1029/2005Tect.00533>.
- Sun, J., Zhu, R., and Bowler, J., 2004, Timing of the Tianshan Mountains uplift constrained by magnetostratigraphic analysis of molasse deposits: *Earth and Planetary Science Letters*, v. 219, p. 239–253, [https://doi.org/10.1016/S0012-821X\(04\)00008-1](https://doi.org/10.1016/S0012-821X(04)00008-1).
- Sun, J.-M., Xu, Q.-H., and Huang, B.-C., 2007, Late Cenozoic magnetochronology and paleoenvironmental changes in the northern foreland basin of the Tianshan Mountains: *Journal of Geophysical Research*, v. 112, p. B04107, <https://doi.org/10.1029/2006JB004653>.
- Sun, J.-M., Li, Y., Zhang, Z.-Q., and Fu, B.-H., 2009, Magnetostriatigraphic data on Neogene growth folding in the foreland basin of the southern Tianshan Mountains: *Geology*, v. 37, p. 1051–1054, <https://doi.org/10.1130/G30278A.1>.
- Sundell, K.E., Taylor, M.H., Styron, R.H., Stockli, D.F., Kapp, P., Hager, C., Liu, D., and Ding, L., 2013, Evidence for constriction and Pliocene acceleration of east-west extension in the North Lunggar rift region of west central Tibet: *Tectonics*, v. 32, p. 1454–1479, <https://doi.org/10.1029/2008Tect.00086>.
- Tapponnier, P., and Molnar, P., 1977, Active faulting and tectonics in China: *Journal of Geophysical Research. Solid Earth*, v. 82, no. 20, p. 2905–2930, <https://doi.org/10.1029/JB082iB20p02905>.
- Tapponnier, P., Peltzer, G., and Armijo, R., 1986, On the mechanics of the collision between India and Asia, in Coward, M.P., and Ries, A.C., eds., *Collision Tectonics: Geological Society of London, Special Publications*, v. 19, no. 1, p. 113–157, <https://doi.org/10.1144/GSL.SP.1986.019.01.07>.
- Thiede, R.C., Arrowsmith, J.R., Bookhagen, B., McWilliams, M., Sobel, E.R., and Strecker, M.R., 2006, Dome formation and extension in the Tethyan Himalaya, Leo Pargil, northwest India: *Geological Society of America Bulletin*, v. 118, no. 5–6, p. 635–650, <https://doi.org/10.1130/B25872.1>.
- Todrani, A., Zhang, B., Speranza, F., and Chen, S.-Y., 2020, Paleomagnetism of the middle Cenozoic Mula Basin (East Tibet): Evidence for km-scale crustal blocks rotated by midlower crust drag: *Geochemistry, Geophysics, Geosystems*, v. 21, no. 9, <https://doi.org/10.1029/2020GC009225>.
- Tong, Y.-B., Yang, Z.-Y., Jing, X.-Q., Zhao, Y., Li, C.-H., Huang, D.-J., and Zhang, X.-D., 2016, New insights into the Cenozoic lateral extrusion of crustal blocks on the southeastern edge of Tibetan Plateau: Evidence from paleomagnetic results from Paleogene sedimentary strata of the Baoshan Terrane: *Tectonics*, v. 35, p. 2494–2514, <https://doi.org/10.1029/2016TC004221>.
- Tong, Y.-B., Wu, Z.-H., Sun, Y.-J., Yang, Z.-Y., Pei, J.-L., Yang, X.-D., Li, J.-F., and Wang, C.-X., 2020, The interaction of the eastward extrusion of the Songpan-Ganzi Terrane and the crustal rotational movement of the Sichuan Basin since the late Paleogene: Evidence from Cretaceous and Paleogene paleomagnetic data sets of the Sichuan Basin: *Tectonics*, v. 39, no. 2, <https://doi.org/10.1029/2019TC005784>.
- Tong, Y.-B., Yang, Z.-Y., Pei, J.-L., Wang, H., Wu, Z.-H., and Li, J.-F., 2021, Crustal clockwise rotation of the southeastern edge of the Tibetan Plateau since the late Oligocene: *Journal of Geophysical Research: Solid Earth*, v. 126, <https://doi.org/10.1029/2020JB020153>.
- Tran, D., Nguyen, T., Dong, C., Vy, Q., Zuchiewicz, W., and Nguyen, V., 2013, Recent crustal movements of northern Vietnam from GPS data: *Journal of Geodynamics*, v. 69, p. 5–10, <https://doi.org/10.1016/j.jog.2012.02.009>.
- Vernant, P., Bilham, R., Szélága, W., Drupka, D., Kalita, S., Bhattacharyya, A.K., Gaur, V.K., Pelgøy, P., Catlin, R., and Berthet, T., 2014, Clockwise rotation of the Brahmaputra Valley relative to India: Tectonic convergence in the eastern Himalaya, Naga Hills, and Shillong Plateau: *Journal of Geophysical Research. Solid Earth*, v. 119, no. 8, p. 6558–6571, <https://doi.org/10.1002/2014JB011196>.
- Wallis, S., Tsujimori, T., Aoya, M., Kawakami, T., Terada, K., Suzuki, K., and Hyodo, H., 2003, Cenozoic and Mesozoic metamorphism in the Longmenshan orogen: Implications for geodynamic models of eastern Tibet: *Geology*, v. 31, p. 745–748, <https://doi.org/10.1130/G19562.1>.
- Walters, R.J., England, P.C., and Houseman, G.A., 2017, Constraints from GPS measurements on the dynamics of the zone of convergence between Arabia and Eurasia: *Journal of Geophysical Research. Solid Earth*, v. 122, p. 1470–1495, <https://doi.org/10.1002/2016JB013370>.
- Wang, E., and Burchfiel, B., 1997, Interpretation of Cenozoic tectonics in the right-lateral accommodation zone between the Ailao Shan shear zone and the eastern Himalayan syntaxis: *International Geology Review*, v. 39, no. 3, p. 191–219, <https://doi.org/10.1080/0206819709465267>.
- Wang, E., Burchfiel, B., Royden, L., Chen, L., Chen, J., Li, W., and Chen, Z., 1998, Late Cenozoic Xianshuihe-Xiaojiang, Red River, and Dali Fault Systems of Southwestern Sichuan and Central Yunnan, China: *Geological Society of America Special Paper* 327, 108 p., <https://doi.org/10.1130/0-8137-2327-2>.
- Wang, Q., Zhang, P.Z., Freymueller, J.T., Bilham, R., Larson, K.M., Lai, X., You, X., Niu, Z., Wu, J., Li, Y., Liu,

- J., Yang, Z., and Chen, Q., 2001, Present-day crustal deformation in China constrained by Global Positioning System measurements: *Science*, v. 294, p. 574–577, <https://doi.org/10.1126/science.1063647>.
- Wang, S., Fang, X., Zheng, D., and Wang, E., 2009, Initiation of slip along the Xianshuhe fault zone, eastern Tibet, constrained by K/Ar and fission-track ages: *International Geology Review*, v. 51, no. 12, p. 1121–1131, <https://doi.org/10.1080/00206810902945132>.
- Wang, W.-t., Zhang, P.-Z., Kirby, E., Wang, L.-H., Zhang, G.-L., Zheng, D.-W., and Chai, C.-Z., 2011, A revised chronology for Tertiary sedimentation in the Sikouzi basin: Implications for the tectonic evolution of the northeastern corner of the Tibetan Plateau: *Tectonophysics*, v. 505, p. 100–114, <https://doi.org/10.1016/j.tecto.2011.04.006>.
- Wang, Y., Wang, M., Shen, Z., Ge, W., Wang, K., Wang, F., and Sun, J., 2013, Inter-seismic deformation field of the Ganzi-Yushu Fault before the 2010 Mw 6.9 Yushu earthquake: *Tectonophysics*, v. 584, p. 138–143, <https://doi.org/10.1016/j.tecto.2012.03.026>.
- Wang, Y., Zhang, B., Schoenbohm, L.M., Zhang, J., Zhou, R., Hou, J., and Ai, S., 2016, Late Cenozoic tectonic evolution of the Ailao Shan-Red River fault (SE Tibet): Implications for kinematic change during plateau growth: *Tectonics*, v. 35, p. 1969–1988, <https://doi.org/10.1020/2016TC004229>.
- Wessel, P., and Bercovici, D., 1998, Interpolation with spline in tension: A Green's function approach: *Mathematical Geology*, v. 30, no. 1, p. 77–93, <https://doi.org/10.1023/A:1021713421882>.
- Whitehouse, P.L., England, P.C., and Houseman, G.A., 2005, A physical model for the motion of the Sierra Block relative to North America: *Earth and Planetary Science Letters*, v. 237, p. 590–600, <https://doi.org/10.1016/j.epsl.2005.03.028>.
- Wilson, D.S., 1993, Confirmation of the astronomical calibration of the magnetic polarity timescale from sea-floor spreading rates: *Nature*, v. 364, p. 788–790, <https://doi.org/10.1038/364788a0>.
- Wolff, R., Hetzel, R., Dunkl, I., Xu, Q., Bröcker, M., and Anzckiewicz, A.A., 2019, High-Angle Normal Faulting at the Tangra Yumco Graben (Southern Tibet) since ~15 Ma: *The Journal of Geology*, v. 127, no. 1, p. 15–36, <https://doi.org/10.1086/700406>.
- Woodruff, W.H., Jr., Horton, B.K., Kapp, P., and Stockli, D.F., 2013, Late Cenozoic evolution of the Lunggar extensional basin, Tibet: Implications for basin growth and exhumation in hinterland plateaus: *Geological Society of America Bulletin*, v. 125, p. 343–358.
- Wu, Z., Zhang, Y., Hu, D., Zhao, X., and Ye, P., 2008, Quaternary normal faulting and its dynamic mechanism of the Cona-Nariyong Co graben in south-eastern Tibet: *Quaternary Sciences*, v. 28, no. 2, p. 232–242.
- Xu, X., Wen, X., Zheng, R., Ma, W., Song, F., and Yu, G., 2003, Pattern of latest tectonic motion and its dynamics for active blocks in Sichuan-Yunnan region, China: *Science in China*, v. 46, no. 2, p. 210–226.
- Xu, Z., Yang, J., Li, H., Zhang, J., and Wu, C., 2007, Orogenic Plateau: Terrane Amalgamation, Collision and Uplift in the Qinghai-Tibet Plateau: Beijing, China, Beijing Geological Publishing House, 458 p.
- Xu, X., Wen, X., Han, Z., Chen, G., Li, C., Zheng, W., Zhnag, S., Ren, Z., Xu, C., Tan, X., Wei, Z., Wang, M., Ren, J., He, Z., and Liang, M., 2013, Lushan M S7.0 earthquake: A blind reserve-fault event: *Chinese Science Bulletin*, v. 58, no. 28–29, p. 3437–3443, <https://doi.org/10.1007/s11434-013-5999-4>.
- Xue, Z.-H., Martellet, G., Lin, W., Faure, M., Chen, Y., Wei, W., Li, S.-J., and Wang, Q.-C., 2017, Mesozoic crustal thickening of the Longmenshan belt (NE Tibet, China) by imbrication of basement slices: Insights from structural analysis, petrofabric and magnetic fabric studies, and gravity modeling: *Tectonics*, v. 36, p. 3110–3134, <https://doi.org/10.1002/2017TC004754>.
- Yan, D.-P., Zhou, M.-F., Li, S.-B., and Wei, G.-Q., 2011, Structural and geochronological constraints on the Mesozoic-Cenozoic tectonic evolution of the Longmen Shan thrust belt, eastern Tibetan Plateau: *Tectonics*, v. 30, no. 6, <https://doi.org/10.1029/2011TC002867>.
- Yan, M.-D., Van der Voo, R., Fang, X.-M., Parés, J.M., and Rea, D.K., 2006, Paleomagnetic evidence for a mid-Miocene clockwise rotation of about 25° of the Guide Basin area in NE Tibet: *Earth and Planetary Science Letters*, v. 241, p. 234–247, <https://doi.org/10.1016/j.epsl.2005.10.013>.
- Yoshioka, S., Liu, Y.Y., Sato, K., Inokuchi, H., Su, L., Zaman, H., and Otofuji, Y., 2003, Paleomagnetic evidence for post-Cretaceous internal deformation of the Chuan Dian Fragment in the Yangtze block: A consequence of indentation of India into Asia: *Tectonophysics*, v. 376, p. 61–74, <https://doi.org/10.1016/j.tecto.2003.08.010>.
- Zhang, H., Osokin, M.E., Liu-Zeng, J., Zhang, P., Reiners, P.W., and Xiao, P., 2016, Pulsed exhumation of interior eastern Tibet: Implications for relief generation mechanisms and the origin of high-elevation planation surfaces: *Earth and Planetary Science Letters*, v. 449, p. 176–185, <https://doi.org/10.1016/j.epsl.2016.05.048>.
- Zhang, P., 2013, Beware of slowly slipping faults: *Nature Geoscience*, v. 6, p. 323–324.
- Zhang, P., Shen, Z., Wang, M., Gan, W., Burgmann, R., Molnar, P., Wang, Q., Niu, Z., Sun, J., Wu, J., Sun, H., and You, X., 2004, Continuous deformation of the Tibetan Plateau from global positioning system data: *Geology*, v. 32, p. 809–812, <https://doi.org/10.1130/G20554.1>.
- Zhang, P.-Z., Wen, X.-Z., Shen, Z.-K., and Chen, J.-H., 2010, Oblique, high-angle, listric-reverse faulting and associated development of strain: The Wenchuan earthquake of May 12, 2008, Sichuan, China: *Annual Review of Earth and Planetary Sciences*, v. 38, p. 353–382, <https://doi.org/10.1146/annurev-earth-040809-152602>.
- Zhang, W.-L., Fang, X.-M., Zhang, T., Song, C.-H., and Yan, M.-D., 2020, Eocene rotation of the north-eastern central Tibetan Plateau indicating stepwise compressions and eastward extrusions: *Geophysical Research Letters*, v. 47, no. 17, <https://doi.org/10.1029/2020GL088989>.
- Zheng, D., Zhang, P.Z., Wan, J.L., Yuan, D.Y., Li, C.Y., Yin, G.M., Zhang, G.L., Wang, Z.C., Min, W., and Chen, J., 2006, Rapid exhumation at ~8 Ma on the Liupan Shan thrust fault from apatite fission-track thermochronology: Implications for growth of the northeastern Tibetan Plateau margin: *Earth and Planetary Science Letters*, v. 248, p. 198–208, <https://doi.org/10.1016/j.epsl.2006.05.023>.
- Zhou, R., Ma, S., and Cai, C., 1996, Late Quaternary active feature of the Ganzi-Yushu fault zone: *Earthquake Research in China*, v. 12, no. 3, p. 250–260.
- Zhu, M., Graham, S., and McHargue, T., 2009, The red river fault zone in the Yinggehai Basin, South China Sea: *Tectonophysics*, v. 476, p. 397–417, <https://doi.org/10.1016/j.tecto.2009.06.015>.
- Zubovich, A.V., Wang, X.-Q., Scherba, Y.G., Schelochkov, G.G., Reilinger, R., Reigber, C., Mosienko, O.I., Molnar, P., Michajlow, W., Makarov, V.I., Li, J., Kuzikov, S.I., Herring, T.A., Hamburger, M.W., Hager, B.H., Dang, Y.-M., Bragin, V.D., and Beisenbaev, R.T., 2010, GPS velocity field for the Tien Shan and surrounding regions: *Tectonics*, v. 29, <https://doi.org/10.1029/2010TC002772>.

SCIENCE EDITOR: BRAD S. SINGER

ASSOCIATE EDITOR: MASSIMO MATTEI

MANUSCRIPT RECEIVED 5 FEBRUARY 2021

REVISED MANUSCRIPT RECEIVED 13 MAY 2021

MANUSCRIPT ACCEPTED 10 JUNE 2021

Printed in the USA